NONDISPERSIVE SPECTROSCOPY OF CELESTIAL X-RAY SOURCES

S. Holt
Goddard Space Flight Center

I am going to begin the discussion of spectroscopy aboard the Einstein Observatory. First, I would like to thank the many people here at Marshall to whom we owe such a great debt. It may sound obligatory for us to come up and say these things, but I assure you that the gratitude which the scientists have for the project personnel is truly sincere. They did a magnificent job.

With respect to spectroscopy aboard Einstein, the consortium members took the point of view that if we were going to do the best job we could on X-ray sources, we should really pursue two separate approaches: one to take advantage of the highest possible resolution we could obtain with dispersive techniques, and two, to take advantage of the maximum amount of area possible, because many X-ray sources are just too dim for us to successfully use the resolution possible with dispersive techniques.

Table 1 indicates what the prospects were prior to the launch of the observatory for doing spectroscopy. The first column lists, in very broad categories, the various flavors of X-ray sources which we knew about (exotic binaries mean binaries which have neutron stars or potential black holes within them). The column labelled $L_x/L_\odot$ is the logarithm of the X-ray luminosity relative to the total luminosity from the Sun. The Sun, in fact, would be -6 on this scale because its X-ray luminosity is only about 1 millionth of its total luminosity. The middle column exemplifies the high efficiency we had to attain to do spectroscopy on a large number of sources. Shown there is the logarithm of the counting rate resulting from a detector with a gross area of 100 cm^2 and 100 percent efficiency (typical of what we can get from Einstein). Most of the sources we expected to look at would give us something like 1 count per second with such a system. If we were using a dispersive technique, it would approximate 1 count per 1000 sec. The last column, which is particularly relevant for an estimate of how useful spectroscopy might be, is a measure of the temperature of these sources. The temperature of 10^6 deg, which is characteristic of the solar corona, is really too low to see a substantial amount of structure from Einstein. At 10^7 deg (approximately 1 keV) the structure is clearer and elements between neon and calcium are either hydrogenic or helium-like. Therefore we expected extensive cooling in these plasmas from line emission in that energy range. However, once you reach 10^8 deg, or when the logarithm becomes two, all the species of mid-Z elements are completely ionized and are no longer visible. So the best things for us to look at are items in the third column which have an approximate value of 1, corresponding to 10^7 deg.

In addition, however, there might be features other than thermal which might be seen from optically thick or non-thermal sources, such as fluorescent lines or different kinds of spectral features.

Now, having decided to do the nondispersive spectroscopy because of the efficiency advantage it gives, we will discuss the selection of the spectrometer. Shown in Figure 1 are traces of real data obtained with an Fe 55 laboratory source, with a K-capture X-ray of about 6 keV. The first peak is the best resolution we can get with a proportional counter. The center peak is resolution which we can get with a device called a gas scintillator which was not available at the time we designed Einstein, but which is basically just a proportional counter without the last stage of amplification, so the noise from that last stage is suppressed. The peak on the right is what we get from a system which is identical to the one which actually flies aboard Einstein. This is a solid state spectrometer, and the small bump which is just coming out of the gas scintillator spectrum is, in fact, a separate line feature from the Mn 55 which results from the K-capture decay. The reason we decided to use a solid-state spectrometer was simply because it was the best available, but there is a very good reason to be enthusiastic about this kind of resolution, which is about 160 eV FWHM. If we look at the separation between line features that we might expect to see, this is just about what we need to be able to separate those features. Figure 2 shows this full-width half-max resolution compared to expected lines from each of the even-Z elements; shown is the energy of Lyman alpha from each of these hydrogenic ion species, the resonance line from helium-like species of these ions, and K alpha from the neutral atom. As you can see, the resolution is just about typical of the separation for most of the atoms. For thermal plasmas in the neighborhood of a few tens of millions of degrees, we expect to see features like these. In addition, we might see some from the odd-Z elements, which are not quite as abundant. The last feature I want to bring to your attention is that a variety of temperature-dependent L-transitions in iron, which has its K transitions at much higher energy (above 6.5 keV), will be present below about 1.5 keV in any thermal spectra we see.

Figure 3 shows the effective area which we can apply using the Einstein telescope and a very small solid-state detector, much smaller than a square centimeter. We get about 100 cm^2 net from the telescope magnification. Figure 3 was prepared just prior to launch. We have two detectors with the one in standby redundancy having a slightly thicker gold contact on the front surface. The one we actually use is shown by the solid line, but we found out some 6 months prior to launch that we were accumulating water ice on the detector surface, reducing our sensitivity at low energy. To try to do something about it at that time would have meant a delay of probably a year in the launch, so we devised a way to operate around it. It means that we have to give up some fraction of the efficiency of the instrument at the lowest energies, but from about 0.8 keV up, we operate virtually unaffected. So, all things considered, we are quite happy with the way things have turned out. We have lost the ability to look at oxygen, but everything else seems to be all right.

Before talking about the Einstein data, let me show you the last of the HEAO-1 data that you will see today. Figure 4 shows an MED CAS A spectrum with the logarithmic actual raw counts plotted, not corrected for anything or folded backwards through the detector response, but just raw counts as a function of logarithmic energy. You can see that there is a clear indication of iron K emission such as we can typically find with HEAO A-2, but that to the left of the heavy vertical line there are no features which are discernible in the raw data. In fact, if you try to fit the totality of these data, which is what the solid line through the data represents, you find that it is necessary to have at least two temperature components. However, the line contributions at lower energies cannot be seen in the raw data. What we can observe with Einstein is the portion of the spectrum from the heavy vertical line at 4.5 keV leftward, so, let me now show you what we see with the solid state spectrometer (Fig. 5).

There are very obvious features in the raw data which we can ascribe unambiguously to helium-like transitions in silicon and in sulphur, but in addition there are many many more little bumps and wiggles which might look tempting but which in fact are a lot more than that. We do not try to replicate the data by fitting some continuum and then just finding lines to stick in. We actually take models which insist that there be collisional equilibrium in the whole source, so that just choosing the temperature defines the positions of the lines. The magnitudes of the lines are then determined solely by the abundances. I can demonstrate some of the things which I have just said. First, if you use the best two-temperature fit which the computer determines and just throw away all the elements above neon, Figure 6 is the contribution from the lower-Z elements. That is, this is closer to the continuum than are the low points between the line features in the raw data. What I am going to do now is synthesize the data by adding one element at a time. Iron L is responsible for most of the excess at the lowest energies (Fig. 7). Figure 8 adds the contribution from magnesium. Figure 9 accounts for the helium-like and hydrogen-like transitions due to silicon, and I can do the same thing for sulphur in Figure 10. There are still features which are, in fact, unambiguously ascribable to argon and calcium, as you can see from Figure 11. Virtually all the young supernova remnants we have seen, with the exception of the ones (like the Crab) which are never going to snow plow up enough material from the interstellar medium to be thermal X-ray sources, have spectra that look like that in Figure 11. There are about 12 of them now which we have seen.

Figure 12 shows Tycho, which is just one example. Tycho is bigger than our whole field of view (while Cas A just about fills it). So we will be able to look at four quadrants of Tycho and see what the subtle differences in the temperature and the abundances are between them. What we are finding is that in the case of Cas A, the abundances for the mid-Z elements which are due to oxygen burning such as silicon and sulphur are about a factor of 3 higher than solar. We are pretty sure that the trend is correct; we are not so certain, however, that the absolute numerology is correct. The reason for that is that the models we are using are strictly collisional equilibrium models and we are sure in all these cases that we have higher temperature components which are not contributing very much to these lines, but which are necessary for the continuum at higher energy. The second point is that the collisional equilibrium models themselves are in the process of being changed all the time, because more and more detailed atomic physics are going into them which can change the best-fit abundances. The shapes do not change very much but the abundances do, and John Raymond and Barry Smith are both, in fact, working on such refinements right now. I guess I should point out that not all the spectra we see have lines. Figure 13 shows the Crab Nebula, which is very very bright and has no line features whatsoever. This is the raw spectrum once again, and its shape just replicates the detector response to a power law. In this case I felt it was fair to invert the spectrum because there should be no pronounced spectral discontinuities in the source spectrum (Fig. 14). The only features observed are a little dimple at about 1.8 keV which is due to interstellar silicon, and the interstellar medium is responsible for the increasing absorption at lower energies. That is something that we see for almost every object.

Sources other than supernova remnants have exhibited thermal line emission as well, although the line emission is not quite as intense. Figure 15 shows the star Capella; it is only 14 parsecs away and is a G star in a binary system. The lines which can be seen are due predominantly to material at less than 10 million degrees but to get the continuum at high energies, it is necessary to introduce a component which goes out to about 50 million degrees or so. We cannot uniquely specify what the whole range of temperatures is, but we can insist, because of the iron, magnesium, silicon, and sulphur features we see, that there has to be a dominant component below 10^7 degrees, and lesser emission out to at least 30 million degrees.

Quite a different kind of object is M-87 (Fig. 16) which is a giant elliptical galaxy at the center of the Virgo Cluster. Here we fit with a single temperature, but the features are not as apparent because the temperature is much higher. The M-87 fit is to about 20 million degrees, and as we go up in temperature the line features will not only shift to higher energies, corresponding to higher ionization states, but will also become less prominent as the continuum takes a larger responsibility for cooling the source.

Going yet higher in temperature (Fig. 17), NGC 1275, a Seyfert galaxy at the core of the Perseus cluster, has a temperature corresponding to almost 50 million degrees. At 50 million degrees, we should not be able to see any more line features, but in fact the bumps and wiggles which the model demands to get an acceptable Chi-square are at energies prescribed by some contamination from material closer to about 10 million degrees. Finally getting up to higher temperatures, Figure 18 shows dwarf novae which have such high temperatures that we can only measure the flat continuum; they have temperatures corresponding to about 8 kV which is almost 100 million degrees. In the case of SS Cygni, it is difficult to see but in fact there are very slight bumps and wiggles even for temperatures this high, but certainly nothing is very obvious. For EX Hydrae, which has the large fraction of its energy in this very high temperature component, there is much more significant spectral structure. This means that less than 1 percent of the total X-ray energy has to be at a temperature of about 10 million degrees or so to account for these very obvious bumps and wiggles. I don't think that we realized the full significance of that until we started looking at sources which we thought were distinctly nonthermal. For example, Figure 19 is a HEAO A-2 photon spectrum of MK 501, inverted so that you can see that it really does look like a straight line on log-log paper. That is the BL Lac object you have heard quite a bit about this morning. We have got an SSS spectrum from it taken at a different time (Fig. 20) so perhaps the fact that the spectral index is about the same is coincidental because you have already heard that it varies, but this is over a smaller dynamic range. We don't see any line features from Mk 501; it just looks pretty flat, with the low-energy turn-over corresponding to just as much gas as it would take to see the object through the 3×10^{21} or so hydrogen atoms per square centimeter in our own galaxy between us and the object.

In general, we have been disappointed when we have looked at compact extragalactic sources (3C 273 does not have any apparent features either); however, remembering that it takes just a very small contamination in terms of total energy from low temperature stuff to stick out, let's look at Figure 21, which is the spectrum we see from the unusual Seyfert galaxy 3C120. This again is the raw data fit with the best power law that we can get. You can see there is some obvious structure which we can't quite match; in fact, we can't get an acceptable fit at all. What I have shown in Figure 22 is exactly the same continuum just lowered by a few percent to illustrate the possibility that what we are seeing is some lines superposed on that power law spectrum. In fact, if we ask a computer to find the positions of possible lines which could be in there, the results are shown in Figure 23. The most prominent proto-line happens to correspond to exactly the helium-like feature in silicon 13 which we see from most of the thermal sources which we have looked at, red shifted by a Z of 0.033, which is the accepted red-shift of the object. Also found is a feature corresponding to a slightly lower ionization state of sulfur, and the lowest energy feature can't really be associated with anything sensibly at that red shift, but there are ways that we can get it just by suitably absorbing a thermal spectrum. This analysis has not been properly performed yet. We can red shift thermal models properly now, but there are a variety of parameters which are still uncertain, and the final analysis will be performed when all the response function uncertainties are resolved in the production data. But it certainly looks very very tantalizing. What it means is that we might be able, with just an infinitesimal contamination by a thermal component at about 10 million degrees corresponding to a tenth of a percent or a hundredth of a percent (in terms of a total energy) from nonthermal X-ray sources, to unambiguously get their red shifts in X-rays.

There is a source, called Cygnus X-3, which to those of us who have done some spectroscopy in X-rays with proportional counters is sort of our favorite because it has the largest amount of iron line emission. In fact, the iron line emission of Cygnus X-3 alone ranks in the top 30 or so sources in the whole sky, in terms of apparent luminosity. We would have expected then, because we ascribed that emission to fluorescence, that if any object was going to give us the opportunity to observe silicon or sulfur fluorescence, which should be down by about a factor of 20 in equivalent width from what iron is, it would be Cyg X-3. It would take me a long time to explain how we went from the lower trace of Figure 24, which didn't fit at all well, to the top trace (which fits much better). Below about 1.2 kV, we don't see any X-rays at all from the source, and the data points plotted below 1.2 keV just correspond to incompletely collected charge from photons which entered at much higher energy. The spectral feature can be fit quite precisely by insisting that there has to be both fluorescence and a thermal component from sulfur. We have been successful in finding fluorescence from sulfur from Cygnus X-3, but the prospect of doing it for other sources is not too good.

In addition to looking for fluorescence, the more general thing we have been doing with pulsars for a long time now is the phrase you heard this morning called "pulse-phase spectroscopy." Figure 25 shows data, again from the solid state spectrometer, from the pulsar Hercules X-1, which has a period of 1.24 sec. The data all plotted twice for clarity, and the resolution enable us to unambiguously separate the energy ranges chosen. The lowest trace looks identical to pulse profiles which you have seen before from Hercules X-1 from 2 to 6 or 2 to 20 keV. and we have always supposed, based upon looking at those higher energy spectra, that the portion of the main pulse was the closest look we had at what we called the intrinsic pulse. This is because the spectrum of the pulse here was hardest, and we assumed that most of the emission at other phases was due to scattering from lower temperature material surrounding it. If we looked at the hardest energies, therefore, we were seeing something corresponding to the raw pulse, or something close to it. Each of the traces if normalized such that the average value is in the middle, and the total range is from zero to twice the average value. As you can see, the pulse between 1.6 and 4.5 keV is almost 100 percent pulsed. Between 1 and 1.6, it is pulsed at only about half that, but the features correspond very well. At the lowest energies, however, what we had presumed was the hard part of the pulse lines up exactly with where the minimum in the soft flux is. So it looks like our supposition really wasn't too bad, and the maximum in the soft flux corresponds, in fact, to something very close to the minimum in the hard flux.

In summary, then, we think that the higher energy curve is our best measure of the raw pulse; and the lower energy trace arises from reprocessing in the sense that it is probably Compton-scattered near the Alven surface. Looking in a little bit more detail at these spectra, Figure 26 is just the raw spectrum obtained near the maximum in the hard pulse. If we compare that with Figure 27, the spectrum from the same source normalized exactly the same way during the portion of the spectrum where the soft flux is at a maximum, then we see that the two cross at about 1.2 kV. We expect that all the reprocessed emission is x-radiation from which, if we had the sensitivity, we could see fluorescence lines, and we are working very hard trying to find them. The expectation for the equivalent width of these features, particularly from silicon, is less than 10 eV. I think it is premature to talk about whether or not we have detected it because we are still refining our response function, but it looks possible for at least silicon. From anything else I am afraid it doesn't look quite so hopeful.

The last example of preliminary indications of the kind of spectroscopy which we can do shows an attempt to measure interstellar features. Figure 28 displays the spectrum of a transient source, called the Norma transient 1608-52; again the raw counts are plotted, and the dimple near 2 keV is what I would like to call your attention to. It is the silicon absorption feature from the interstellar medium. This feature is completely consistent with the column density to the source, but Figure 29 is apparently fit with exactly the same spectrum. The star with which it has been identified is a highly reddened object which is behind the Coalsack Nebula, so that if any star in the X-ray catalog is going to have more dust in the line of sight relative to the gas in the line of sight, then it is going to be 1258-61. The gas which is implied by the low energy absorption in 1608-52 is just about the same as the gas that it takes to fit 1258-61; however, where there is a very very small dimple in the curve for 1608-52 corresponding to exactly what the model tells us is interstellar absorption due to silicon, in 1258-61 there is, in fact, a much more pronounced dip, at least 3 times more silicon relative to hydrogen as required for 1608-52 and it occurs in exactly the right place, 1.83 kV.

What I have tried to do today is to show you some examples of the kinds of thermal features we see, the kind of nonthermal features we see, and the very exciting possibility of seeing small traces of thermal features in either much higher temperature objects or nonthermal objects. Our analyses are still quite preliminary, and we expect to go once more around the sky before the cryogen disappears, so that we are going to look at those objects which have been most interesting for us the first time to get better statistics, as well as those objects we haven't looked at yet which look like promising candidates for non-dispersive spectroscopy.

TABLE 1. X-RAY SOURCES

Class	"Typical" $\log_{10}$		
	L_x/L_o	$(100\ \text{cm-sec})^{-1}$	T/T_6
Stars	0	<0	0
Dwarf Binaries	1	0	2 (thick)
Supernova Remnants	2	1	1
"Exotic" Binaries	4	2	2 (thick)
Compact Galaxies	11	0	Non-thermal
Clusters of Galaxies	13	0	2

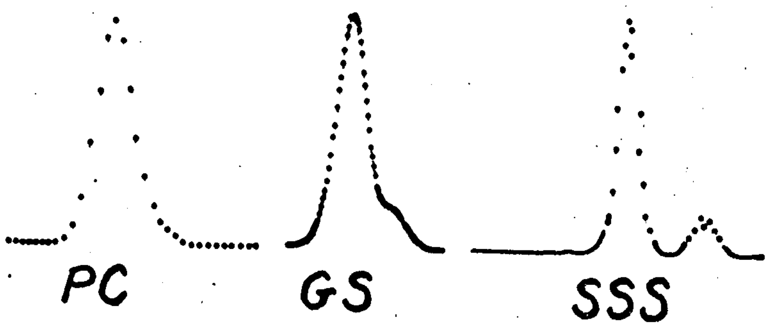

Figure 1

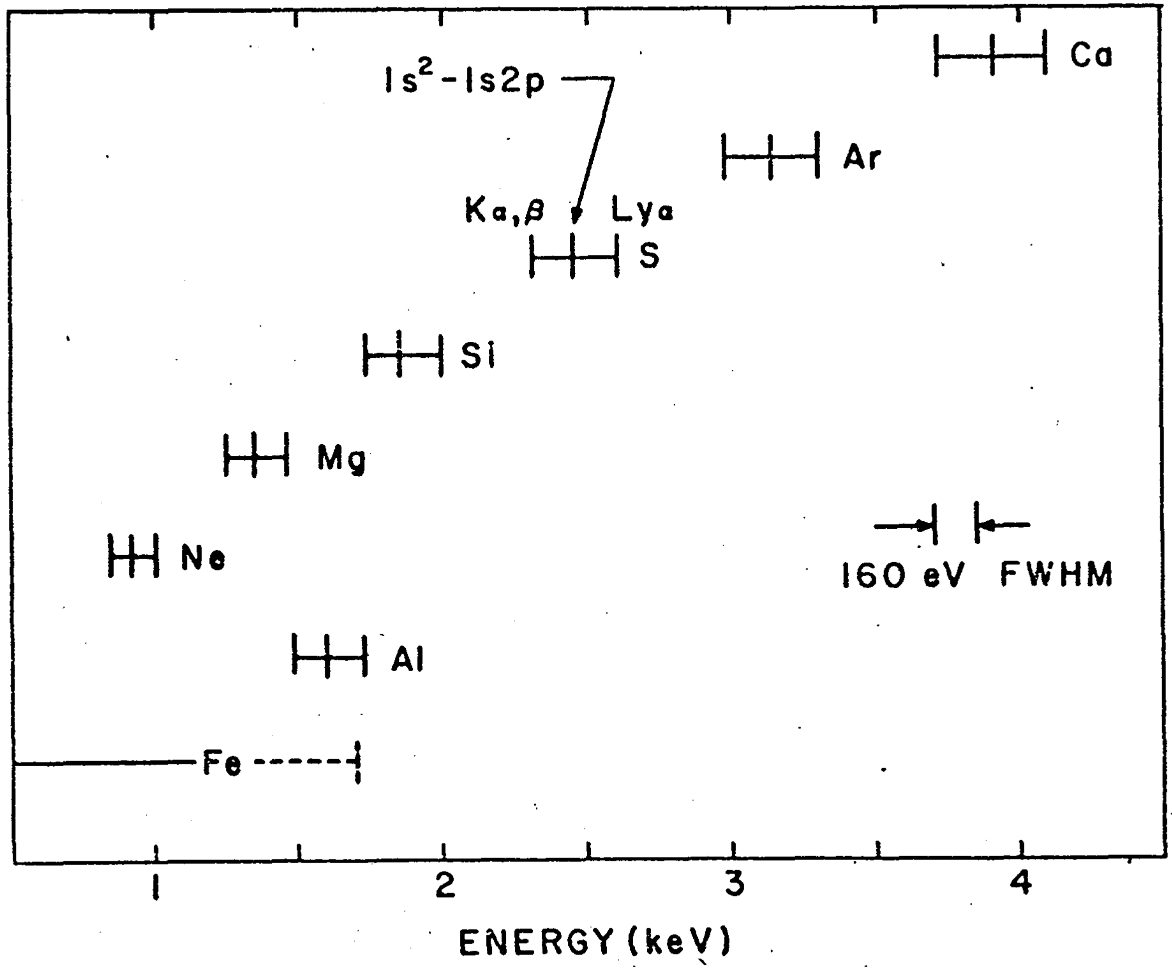

Ca
$1s^2$-1s2p
Ar
Kα,β
Lyα
S
Si
Mg
Ne
160 eV FWHM
Al
Fe
1
2
3
4
ENERGY (keV)

Figure 2

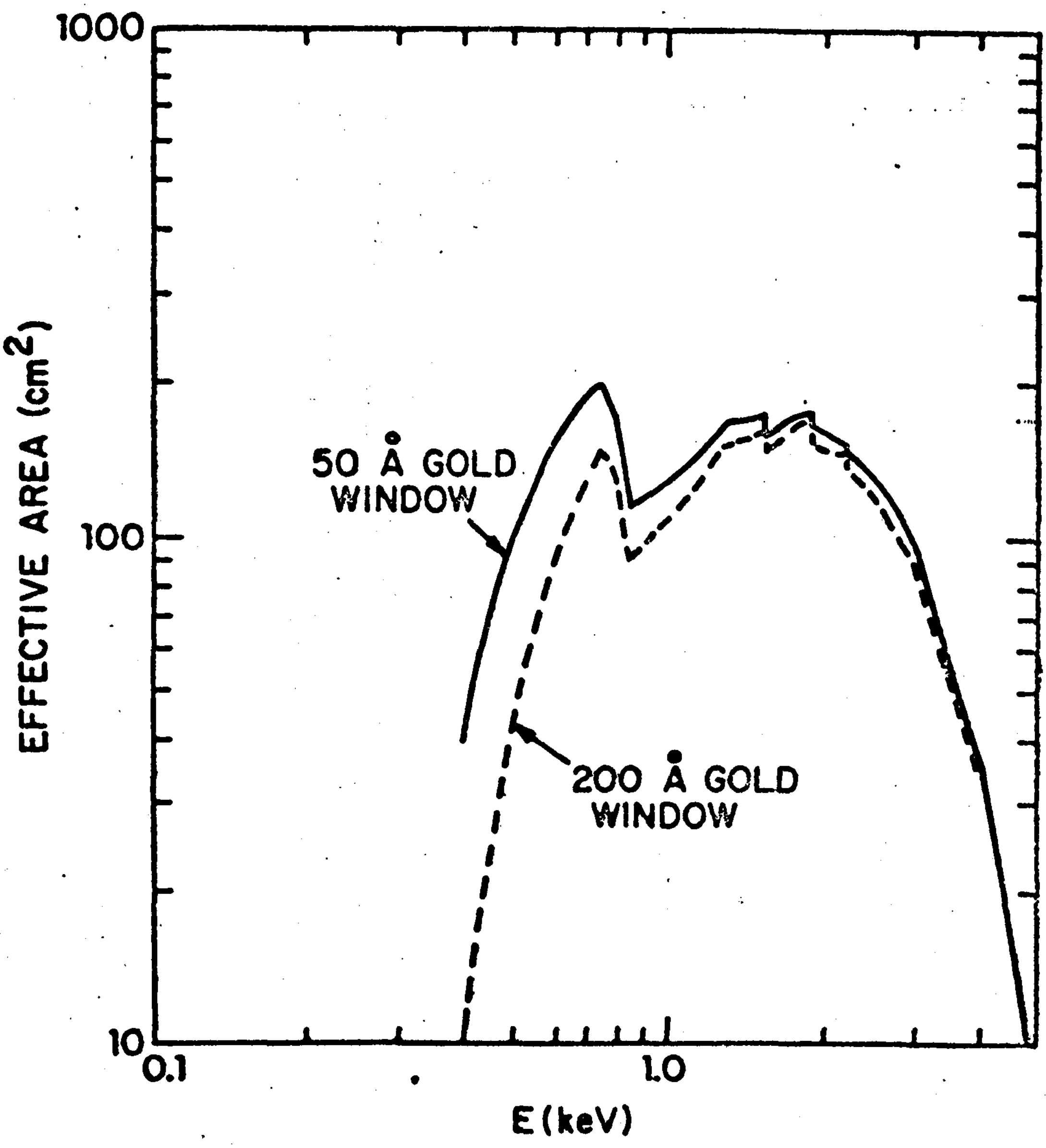

Figure 3. SSS effective area.

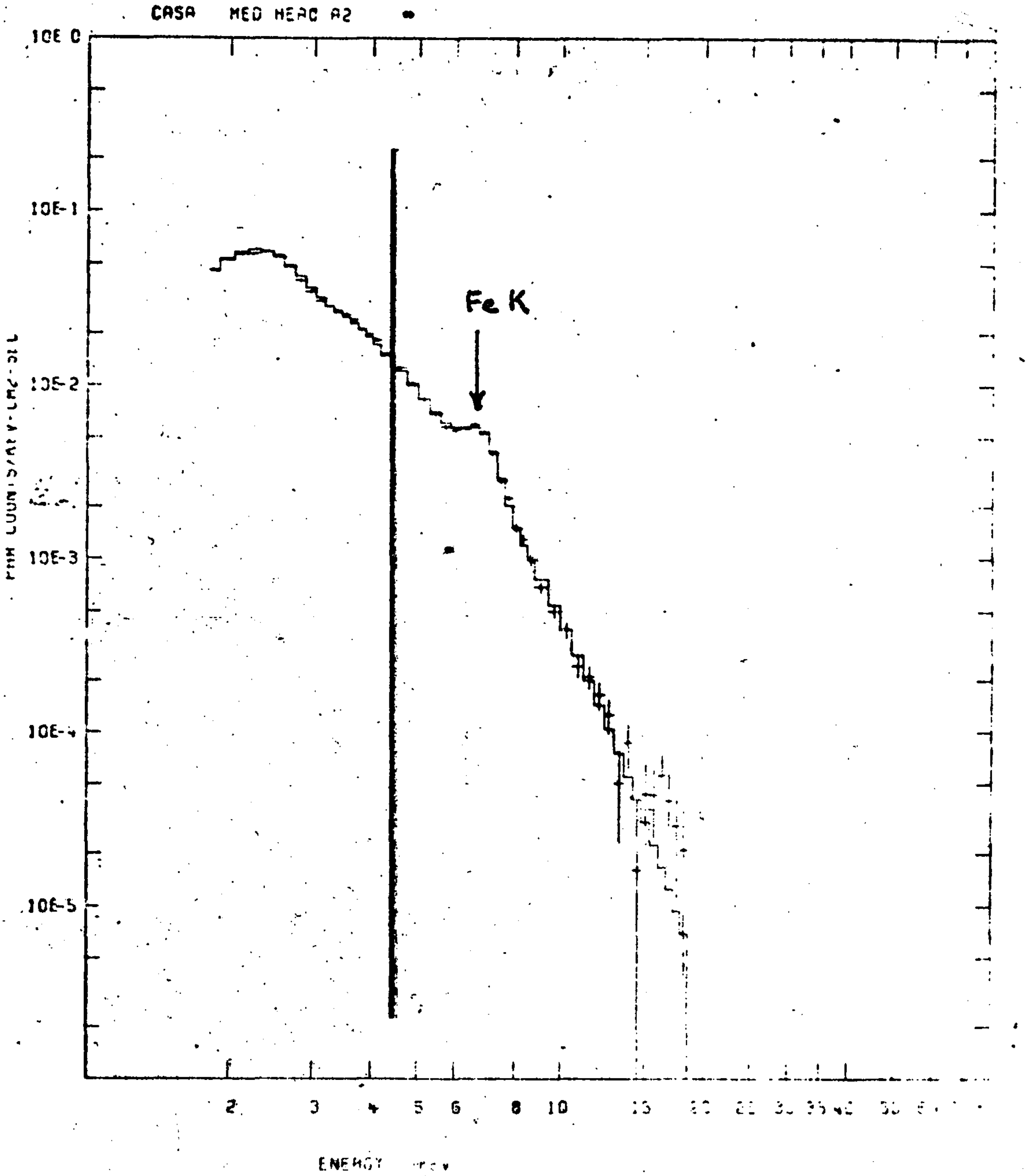
CASA MED HEAO A2
10E 0
10E-1
10E-2
10E-3
10E-4
10E-5
Fe K
2
3
4
5
6
8
10
ENERGY

Figure 4

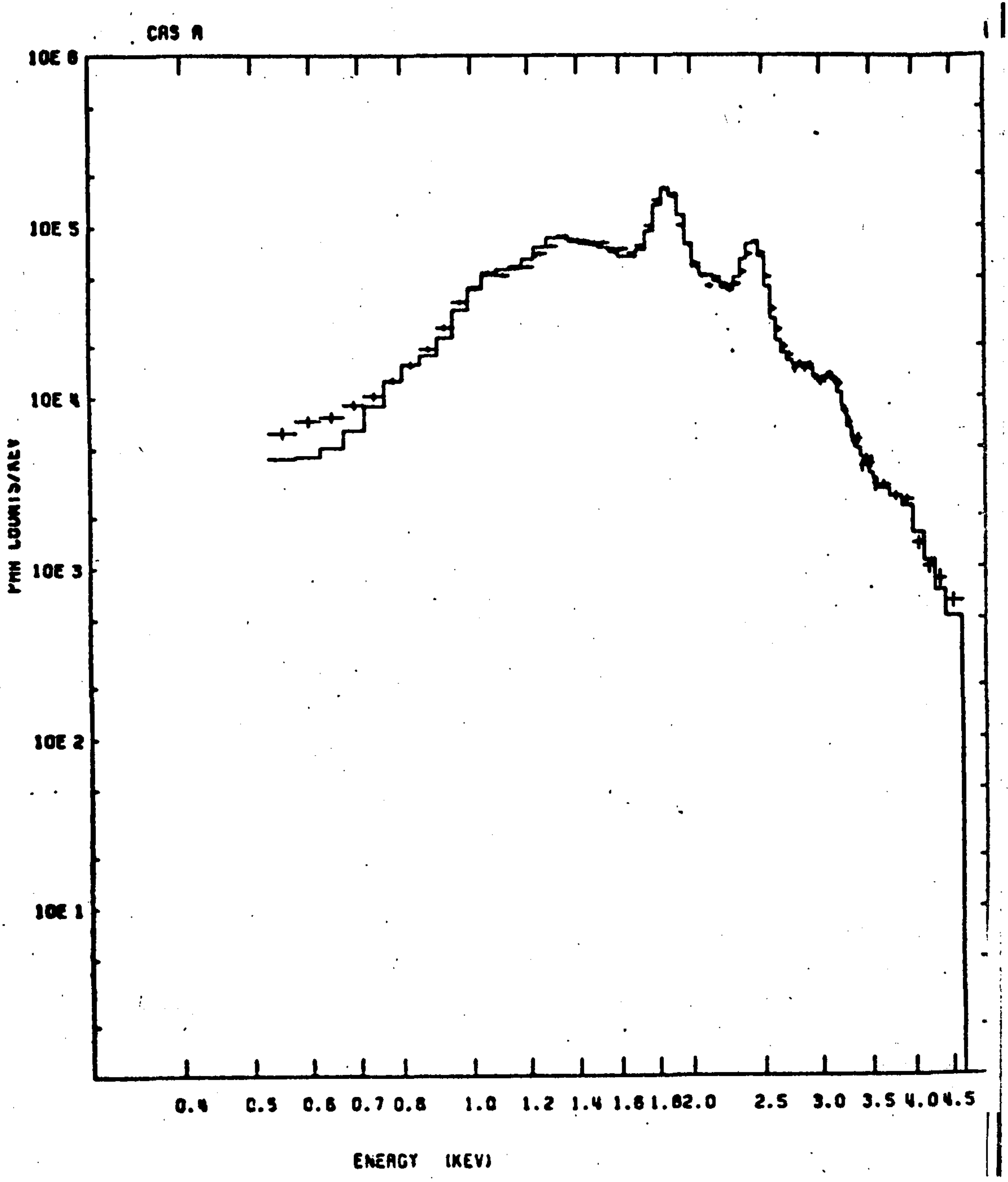
CAS A
10E 6
10E 5
10E 4
10E 3
10E 2
10E 1
PHA COUNTS/KEV
0.4
0.5
0.6
0.7
0.8
1.0
1.2
1.4
1.6
1.8
2.0
2.5
3.0
3.5
4.0
4.5
ENERGY (KEV)

Figure 5

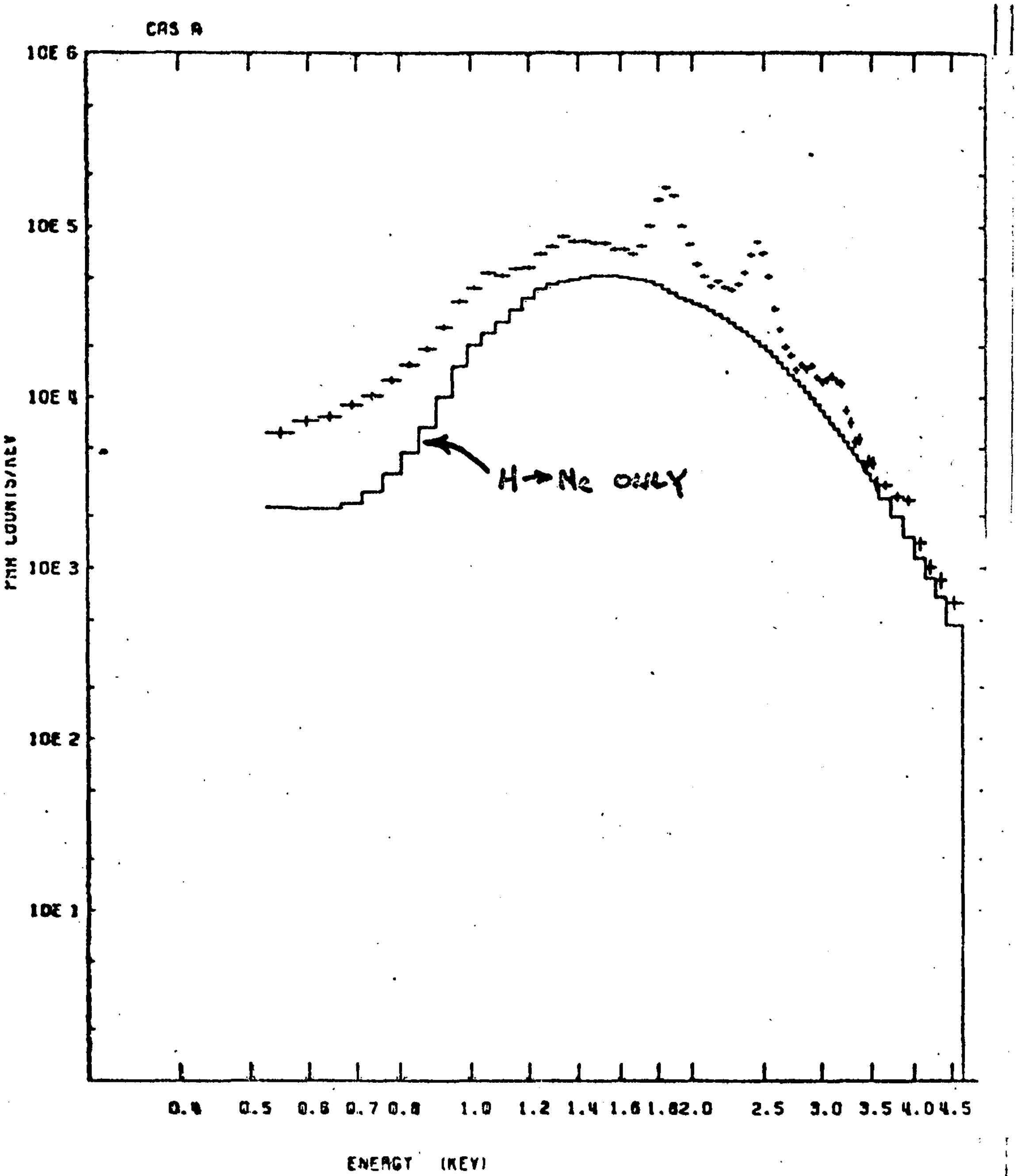

CAS A
10E 6
10E 5
10E 4
10E 3
10E 2
10E 1
PHA COUNTS/KEV
H → Ne ONLY
0.4
0.5
0.6
0.7
0.8
1.0
1.2
1.4
1.6
1.8
2.0
2.5
3.0
3.5
4.0
4.5
ENERGY (KEV)

Figure 6

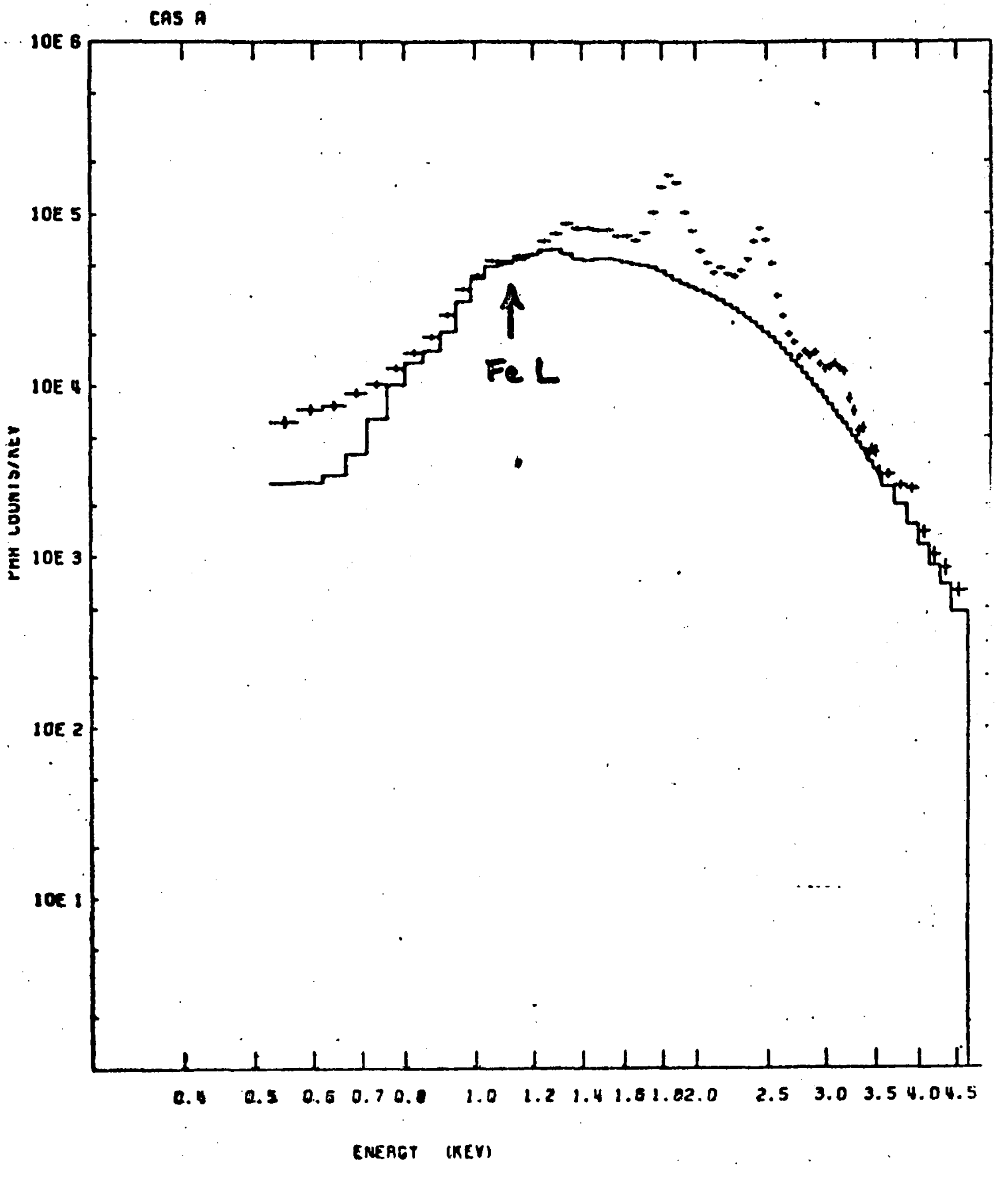
CAS A
10E 6
10E 5
10E 4
10E 3
10E 2
10E 1
PHA COUNTS/KEV
Fe L
0.4 0.5 0.6 0.7 0.8 1.0 1.2 1.4 1.6 1.8 2.0 2.5 3.0 3.5 4.0 4.5
ENERGY (KEV)

Figure 7

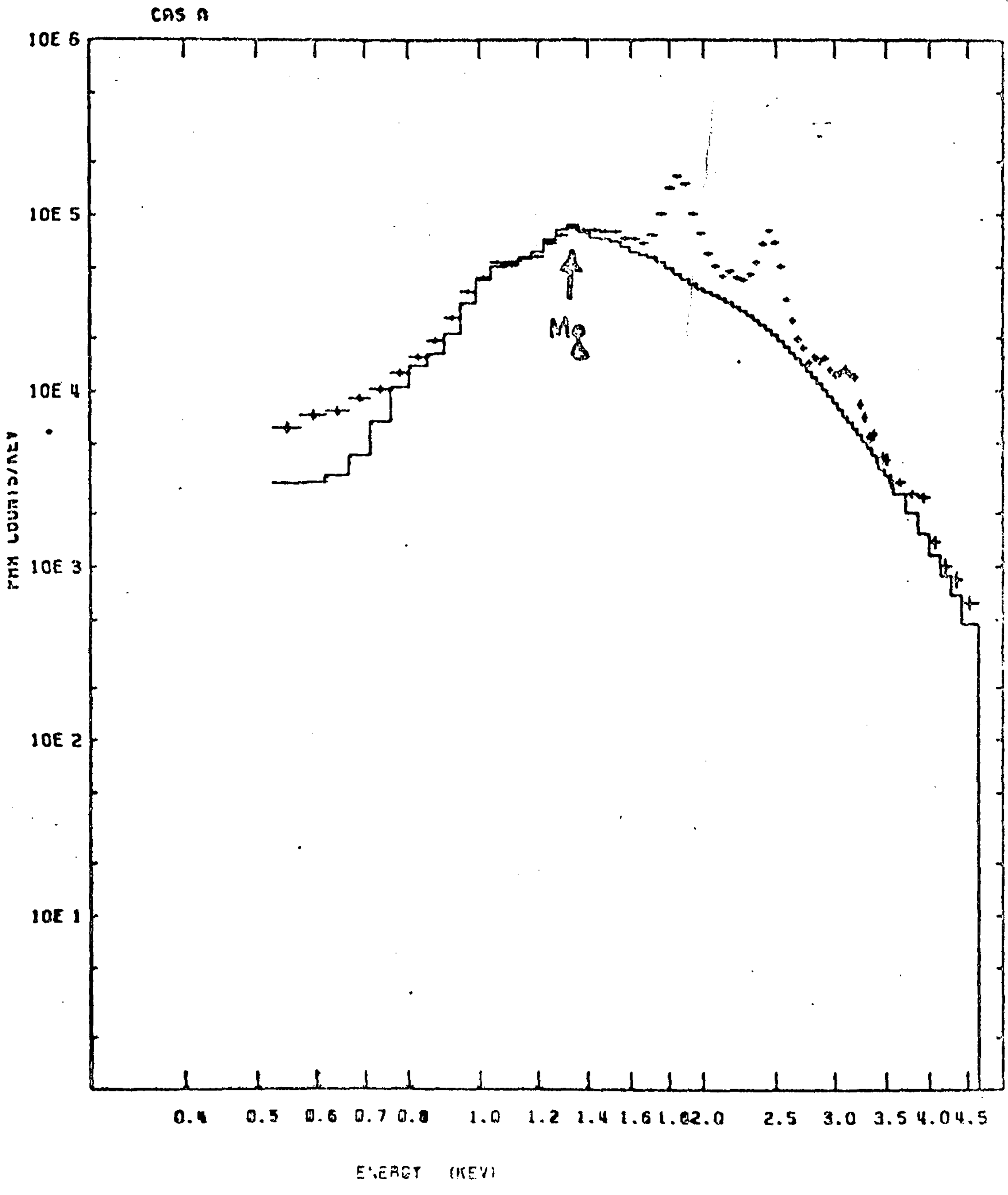
CAS A
10E 6
10E 5
10E 4
10E 3
10E 2
10E 1
Mg
0.4 0.5 0.6 0.7 0.8 1.0 1.2 1.4 1.6 1.8 2.0 2.5 3.0 3.5 4.0 4.5
ENERGY (KEV)

Figure 8

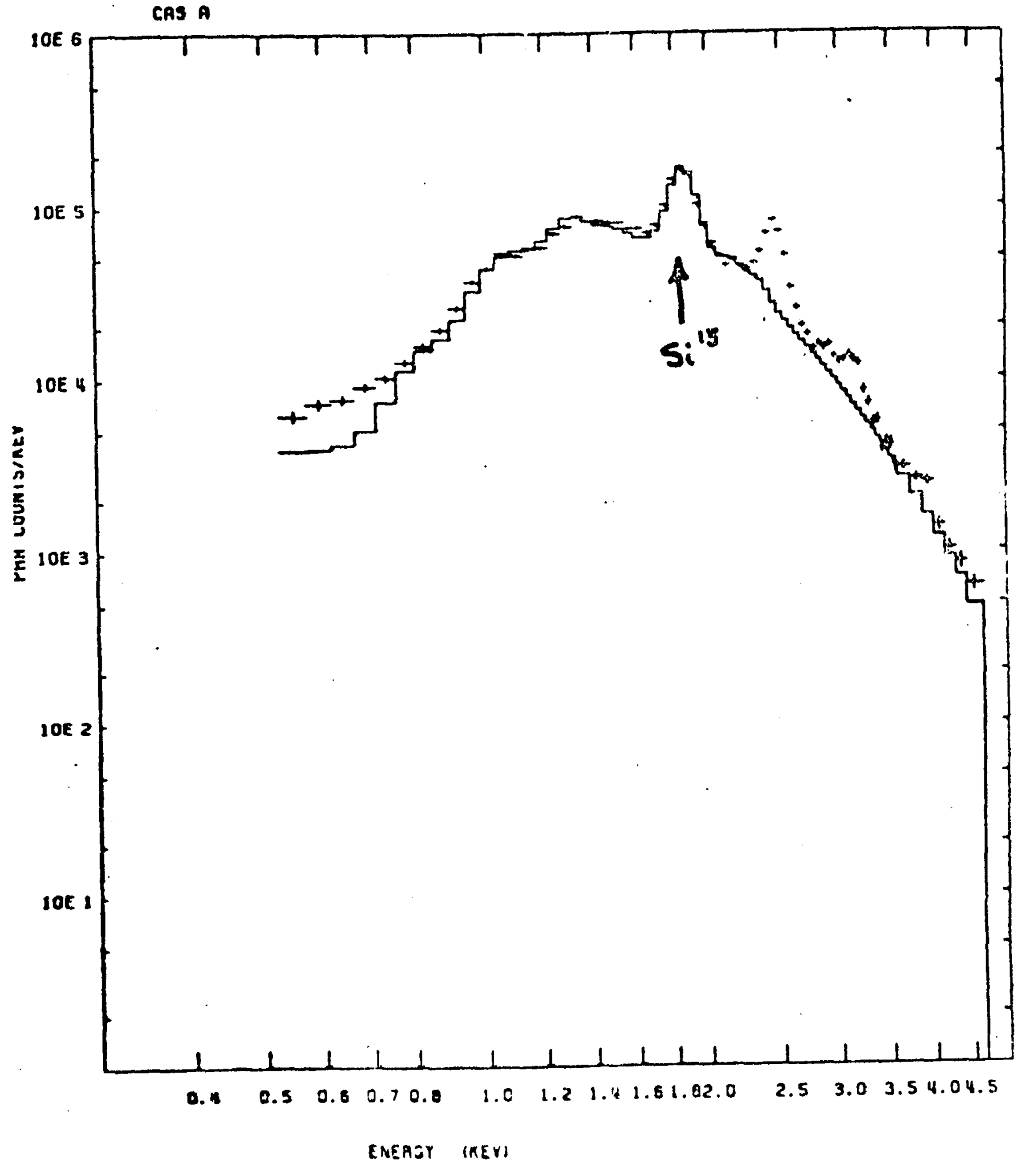
CAS A
10E 6
10E 5
10E 4
10E 3
10E 2
10E 1
PHA COUNTS/KEV
Si^{15}
0.4 0.5 0.6 0.7 0.8 1.0 1.2 1.4 1.6 1.8 2.0 2.5 3.0 3.5 4.0 4.5
ENERGY (KEV)

Figure 9

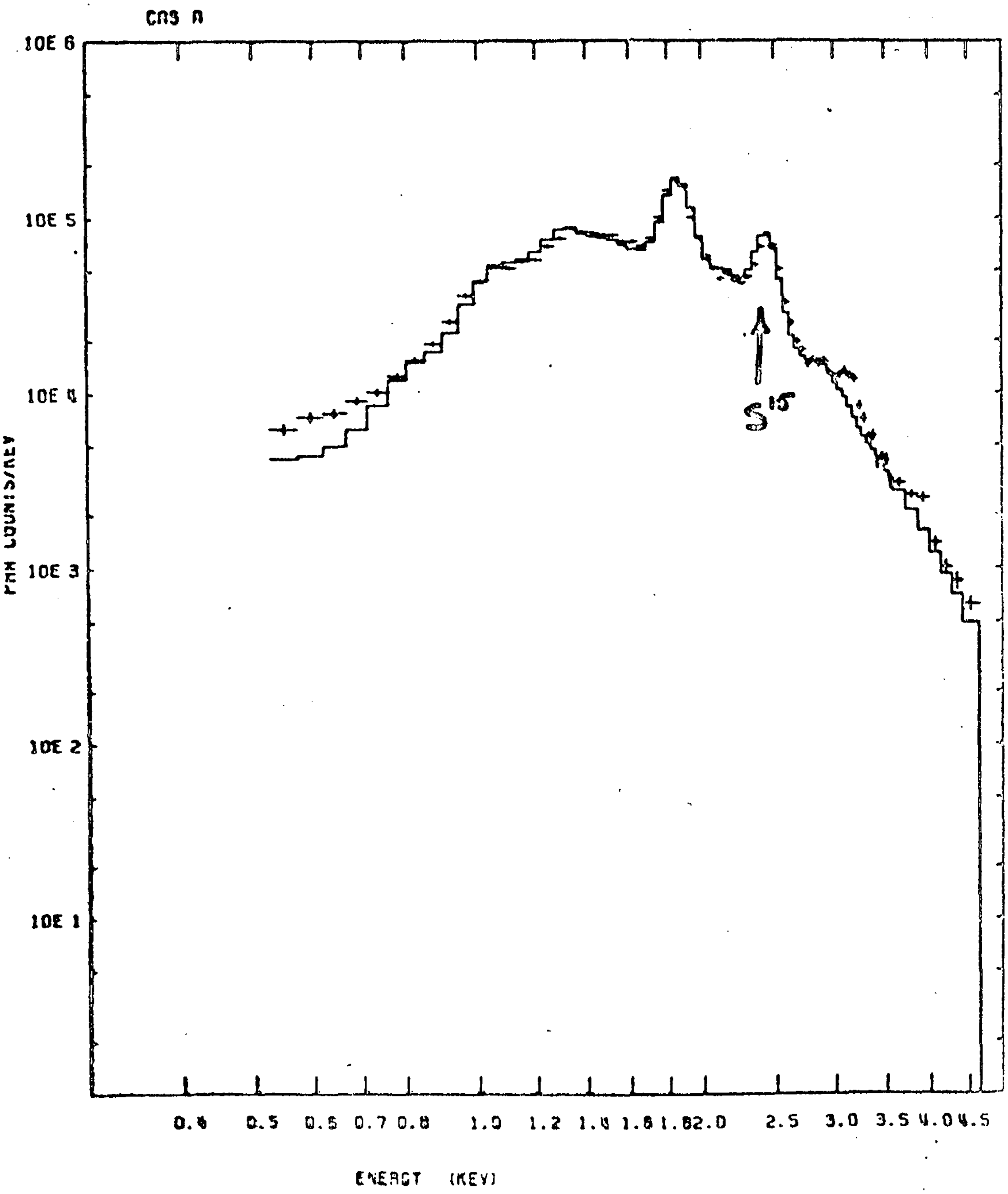
CAS A
10E 6
10E 5
10E 4
10E 3
10E 2
10E 1
PHA COUNTS/KEV
1.0
1.2
2.5
3.0
ENERGY (KEV)

Figure 10

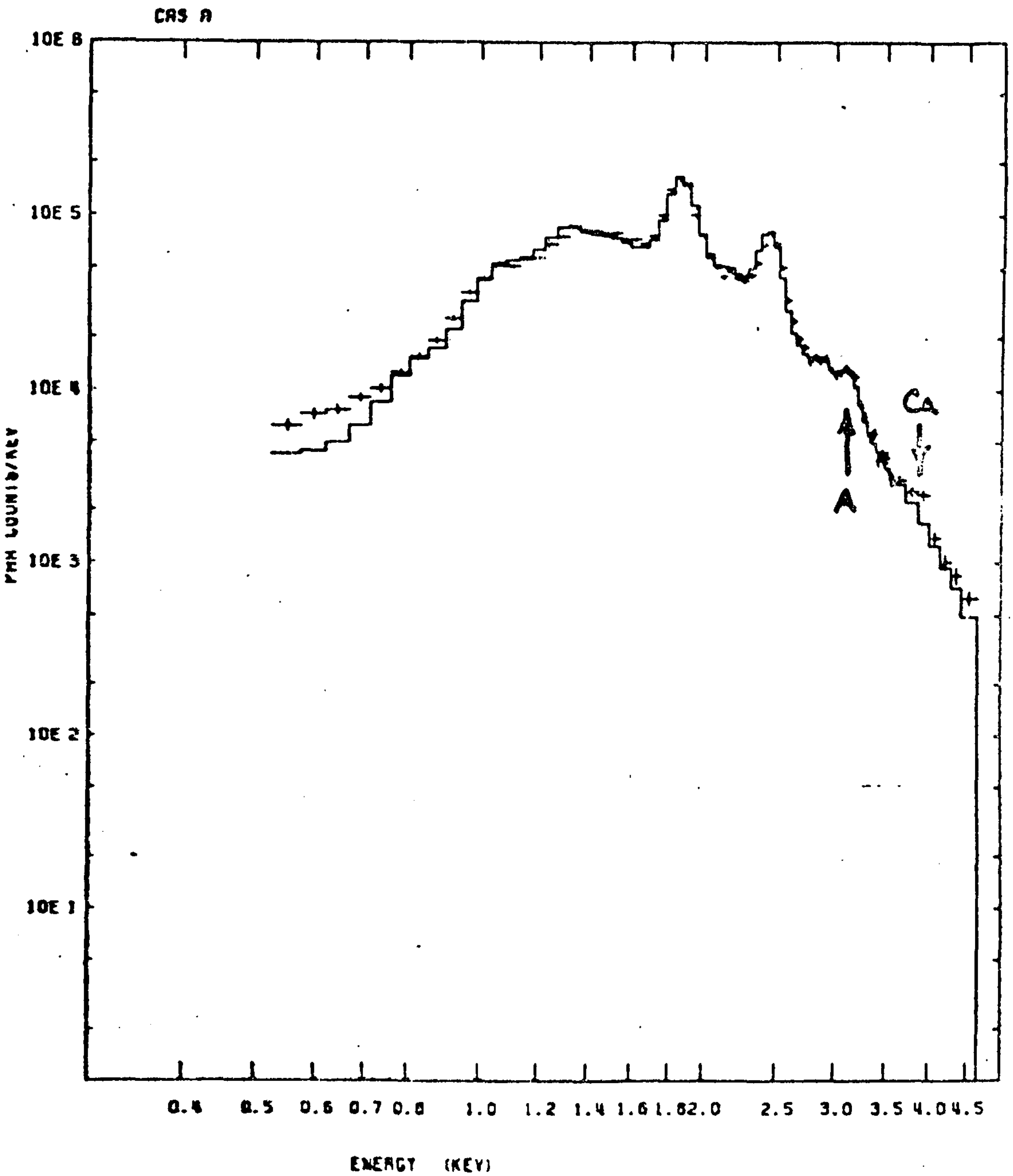
CAS A
10E 6
10E 5
10E 4
10E 3
10E 2
10E 1
PHA COUNTS/KEV
Ca
A
0.4
0.5
0.6
0.7
0.8
1.0
1.2
1.4
1.6
1.8
2.0
2.5
3.0
3.5
4.0
4.5
ENERGY (KEV)

Figure 11

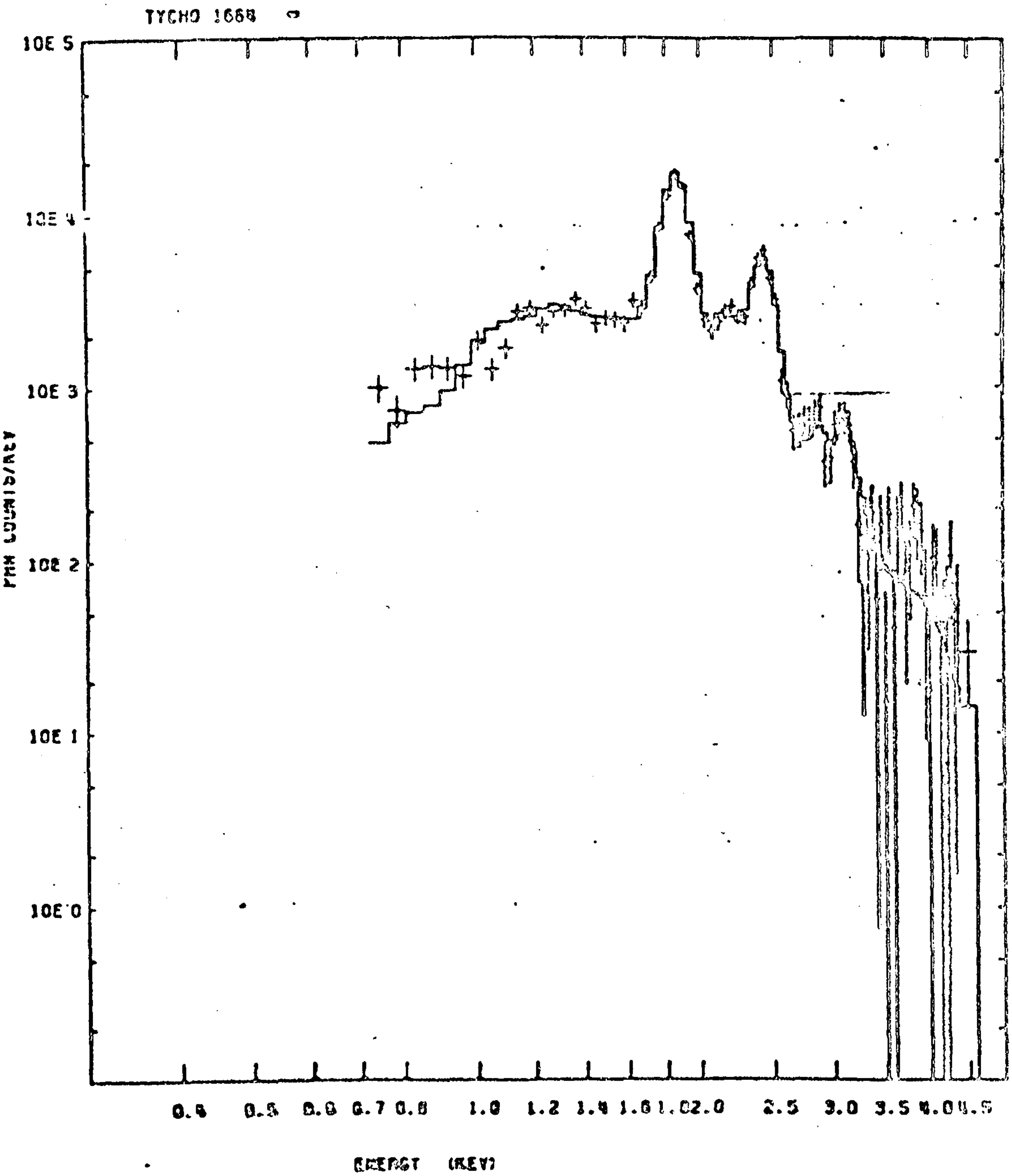

TYCHO 1668
10E 5
10E 4
10E 3
10E 2
10E 1
10E 0
PHA COUNTS/KEV
0.4
0.5
0.6
0.7
0.8
1.0
1.2
1.4
1.6
1.8
2.0
2.5
3.0
3.5
4.0
4.5
ENERGY (KEV)

Figure 12

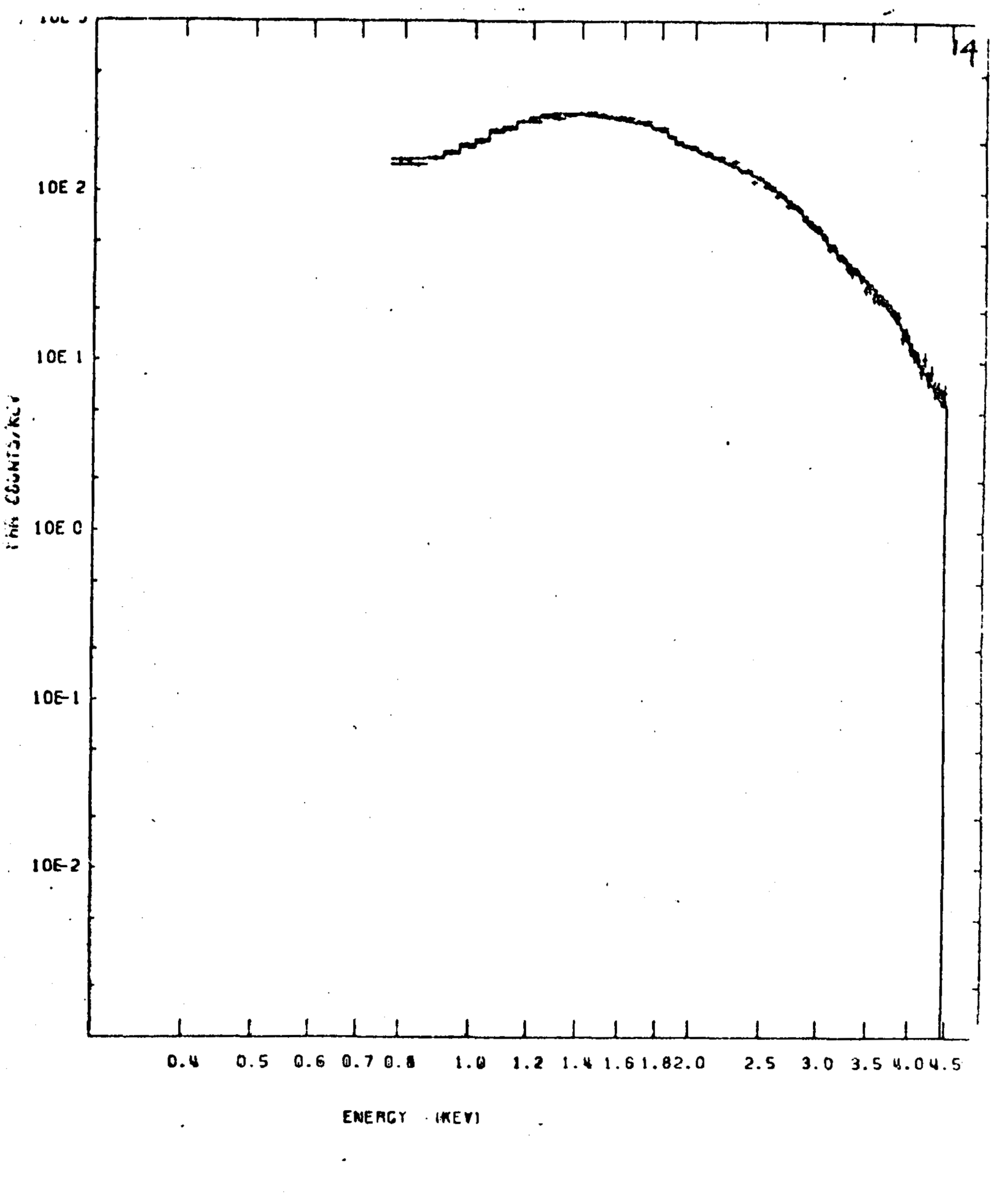
10E 2
10E 1
10E 0
10E-1
10E-2
0.4
0.5
0.6
0.7
0.8
1.0
1.2
1.4
1.6
1.8
2.0
2.5
3.0
3.5
4.0
4.5
ENERGY (KEV)
14

Figure 13

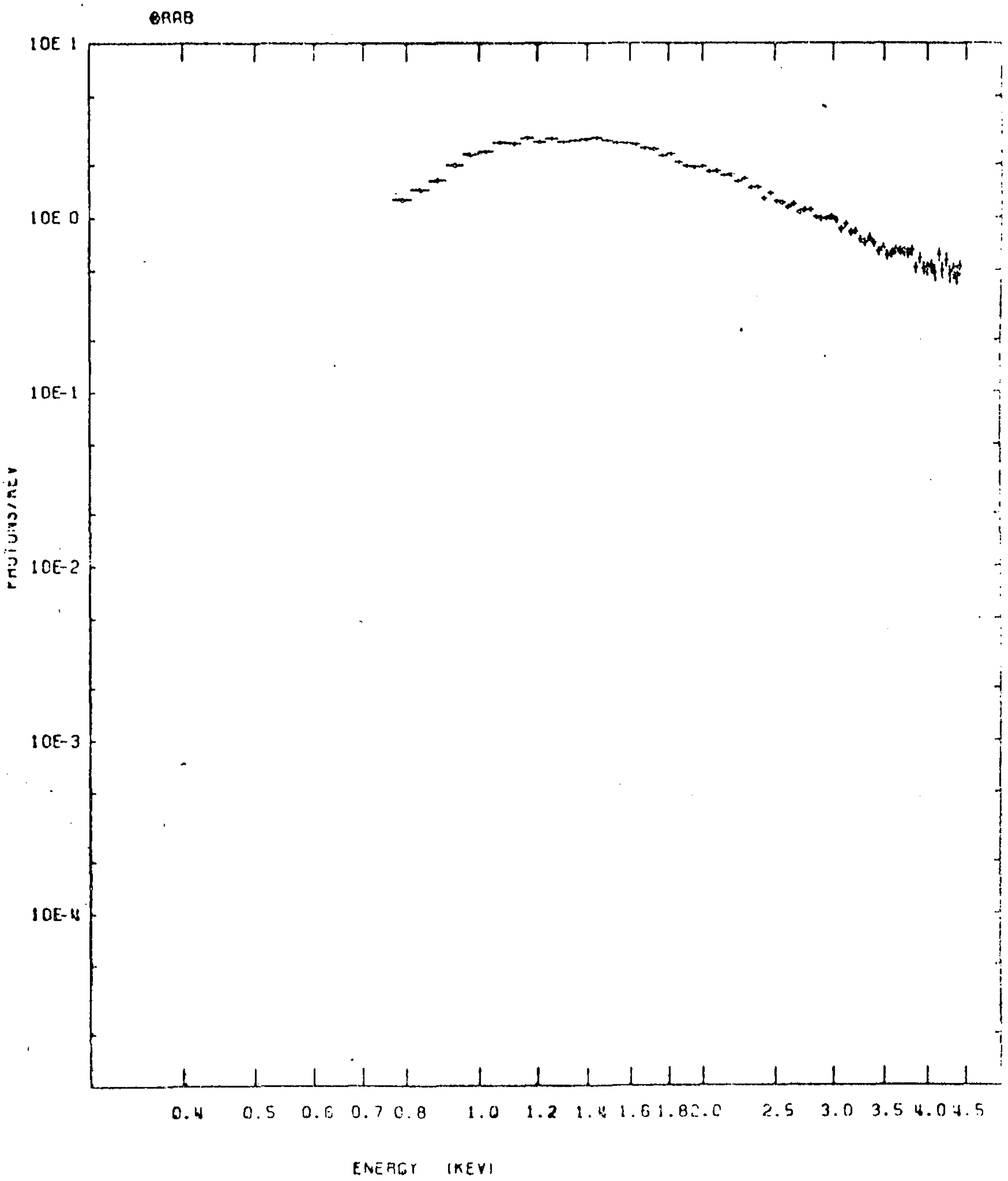
CRAB
10E 1
10E 0
10E-1
10E-2
10E-3
10E-4
PHOTONS/KEV
0.4
0.5
0.6
0.7
0.8
1.0
1.2
1.4
1.6
1.8
2.0
2.5
3.0
3.5
4.0
4.5
ENERGY (KEV)

Figure 14

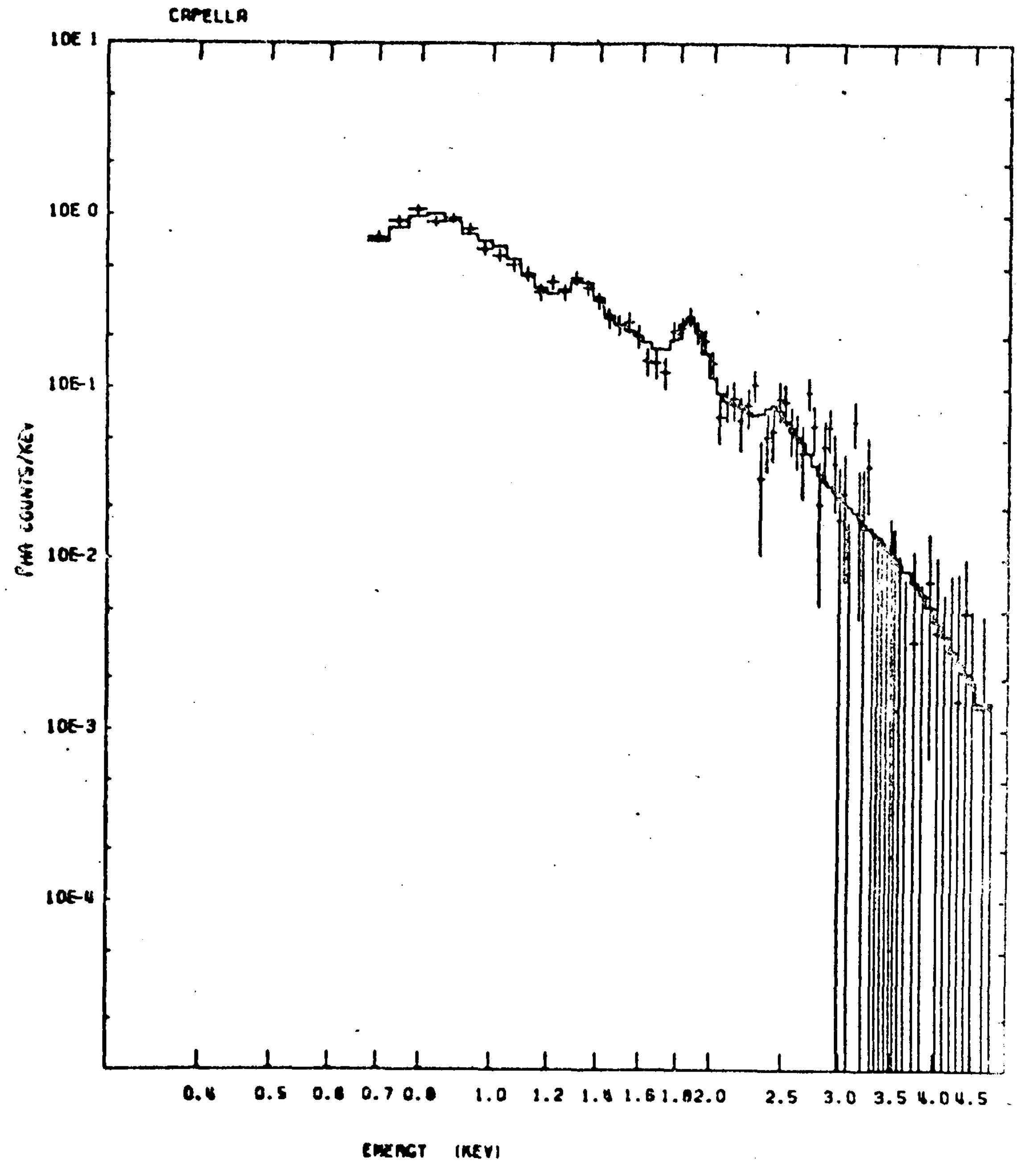

CAPELLA
10E 1
10E 0
10E-1
10E-2
10E-3
10E-4
PHA COUNTS/KEV
0.4 0.5 0.6 0.7 0.8 1.0 1.2 1.4 1.6 1.8 2.0 2.5 3.0 3.5 4.0 4.5
ENERGY (KEV)

Figure 15

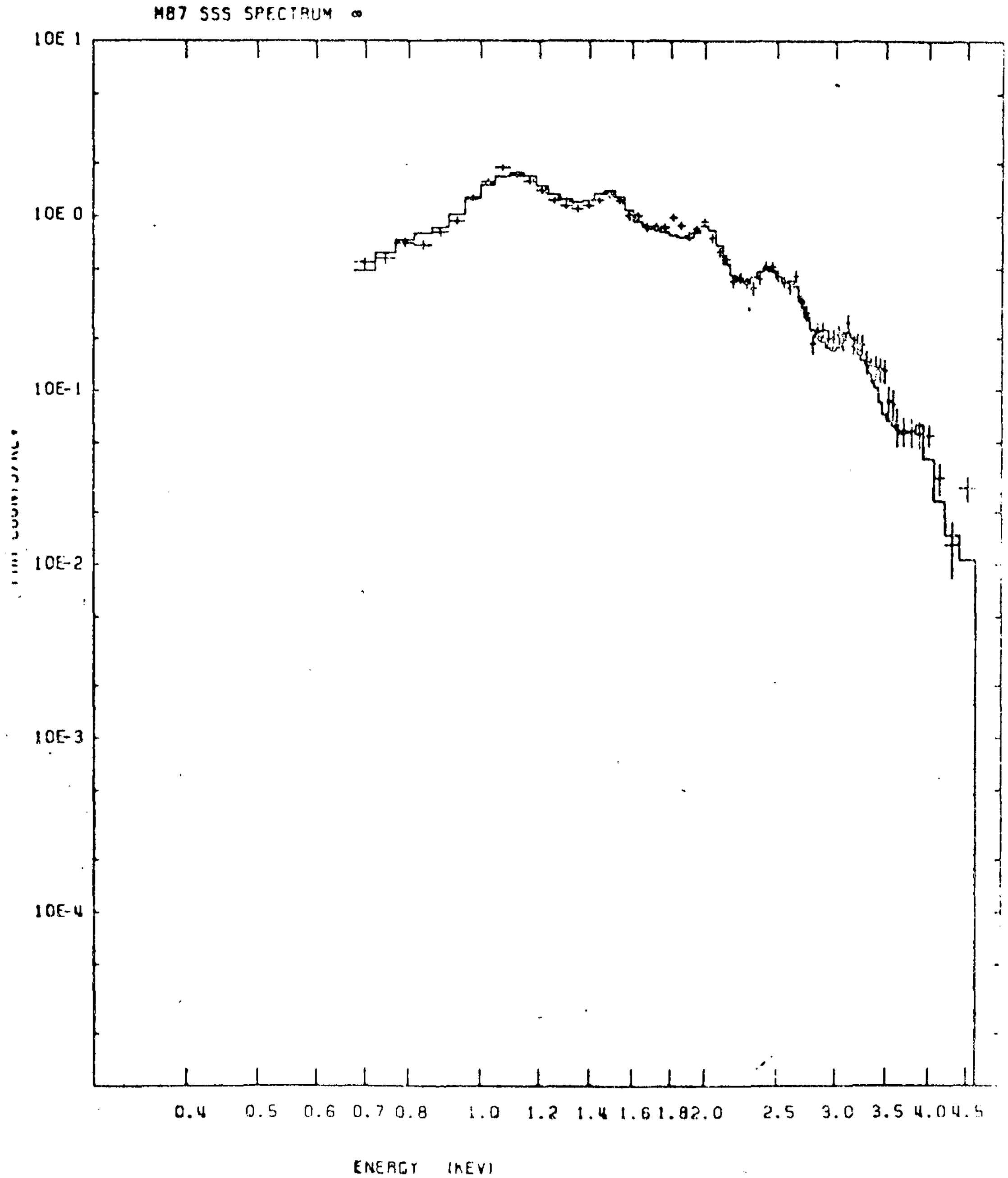
M87 SSS SPECTRUM
10E 1
10E 0
10E-1
10E-2
10E-3
10E-4
0.4
0.5
0.6
0.7
0.8
1.0
1.2
1.4
1.6
1.8
2.0
2.5
3.0
3.5
4.0
4.5
ENERGY (KEV)

Figure 16

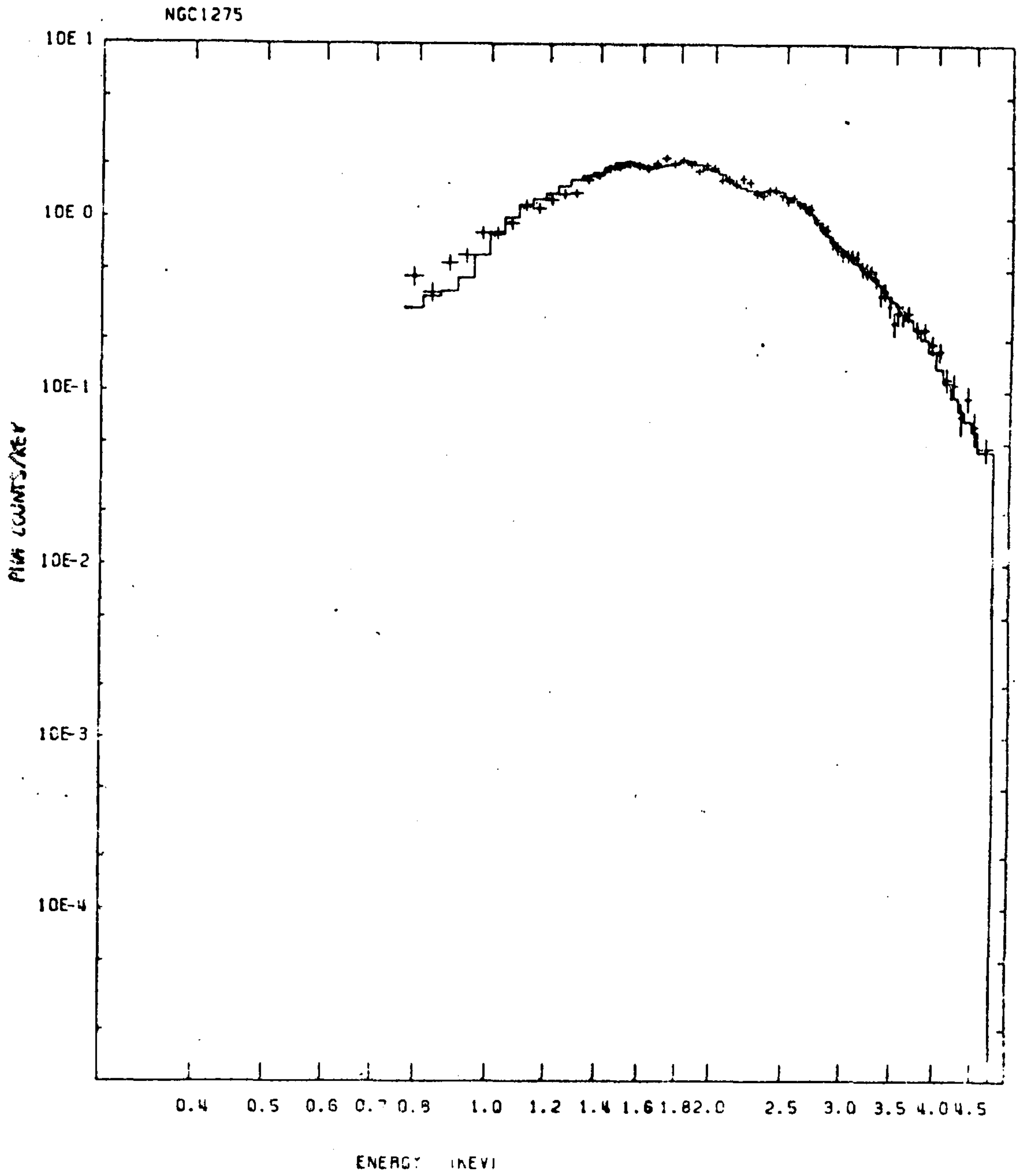
NGC1275
10E 1
10E 0
10E-1
10E-2
10E-3
10E-4
PHA COUNTS/KEV
0.4
0.5
0.6
0.8
1.0
1.2
1.4
1.6
1.8
2.0
2.5
3.0
3.5
4.0
4.5
ENERGY (KEV)

Figure 17

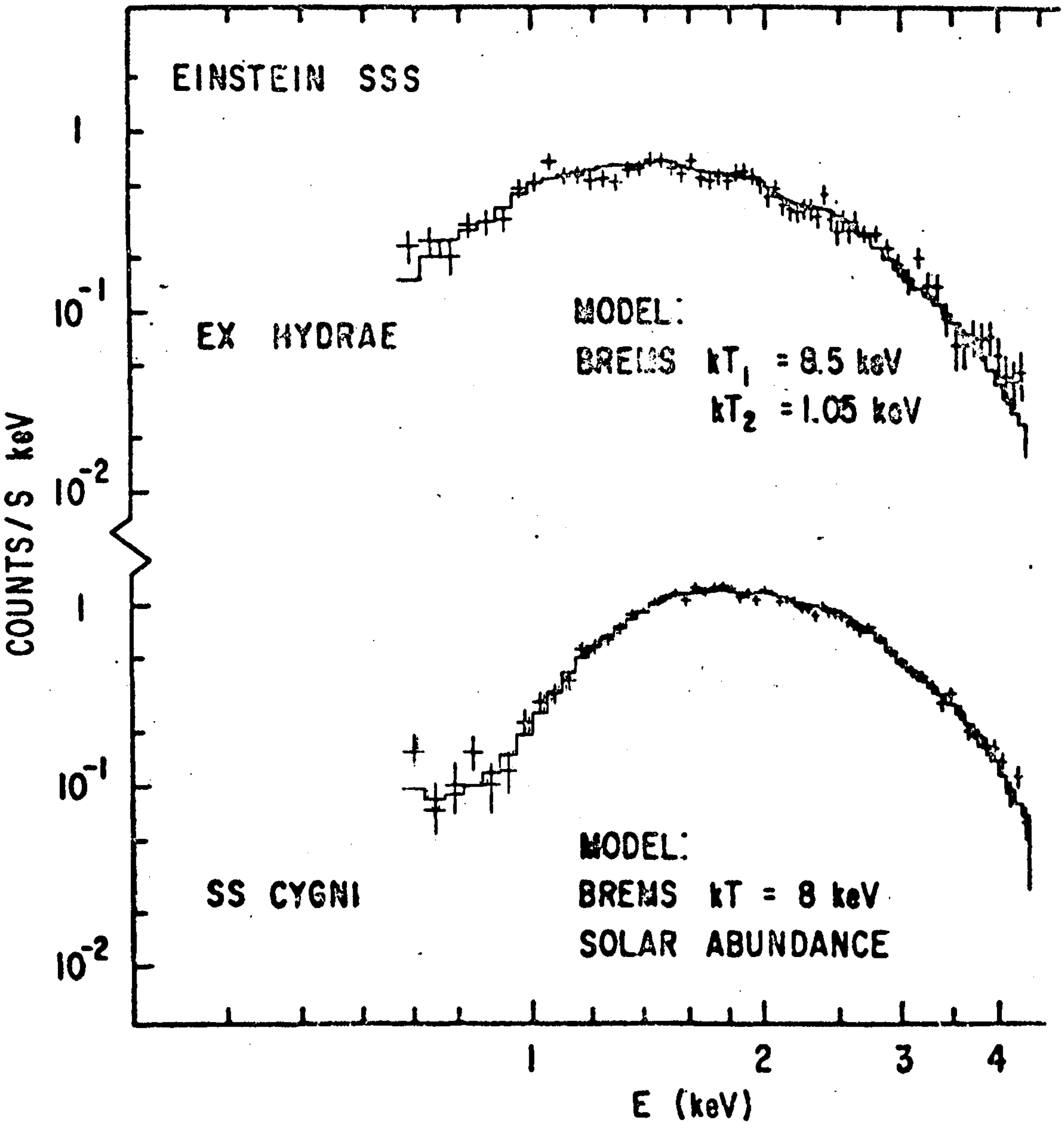
EINSTEIN SSS
EX HYDRAE
MODEL:
BREMS kT1 = 8.5 keV
kT2 = 1.05 keV
SS CYGNI
MODEL:
BREMS kT = 8 keV
SOLAR ABUNDANCE
COUNTS/S keV
E (keV)
1
10-1
10-2
1
10-1
10-2
1
2
3
4

Figure 18

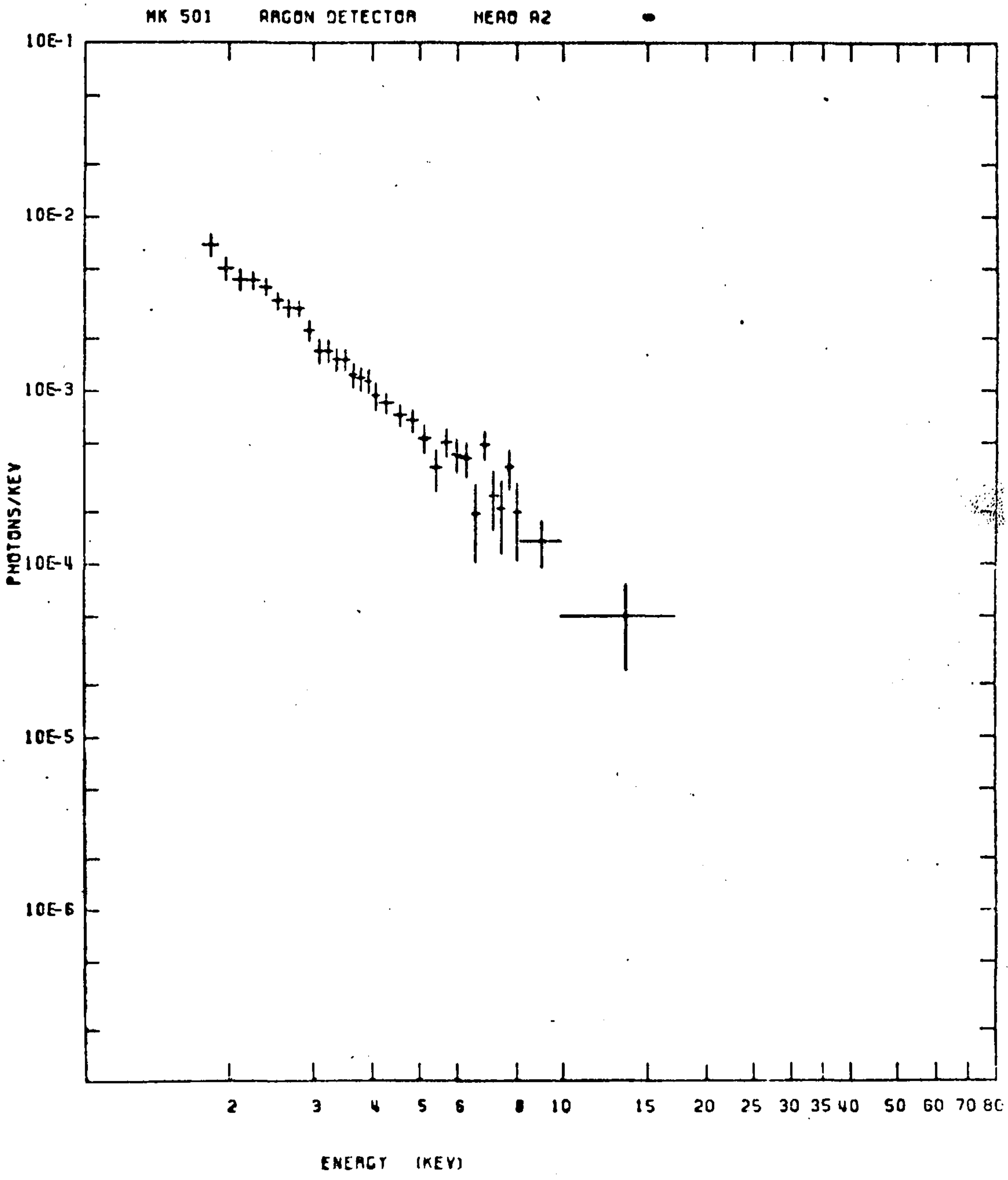
MK 501 ARGON DETECTOR HEAO A2
PHOTONS/KEV
10E-1
10E-2
10E-3
10E-4
10E-5
10E-6
2 3 4 5 6 8 10 15 20 25 30 35 40 50 60 70 80
ENERGY (KEV)

Figure 19

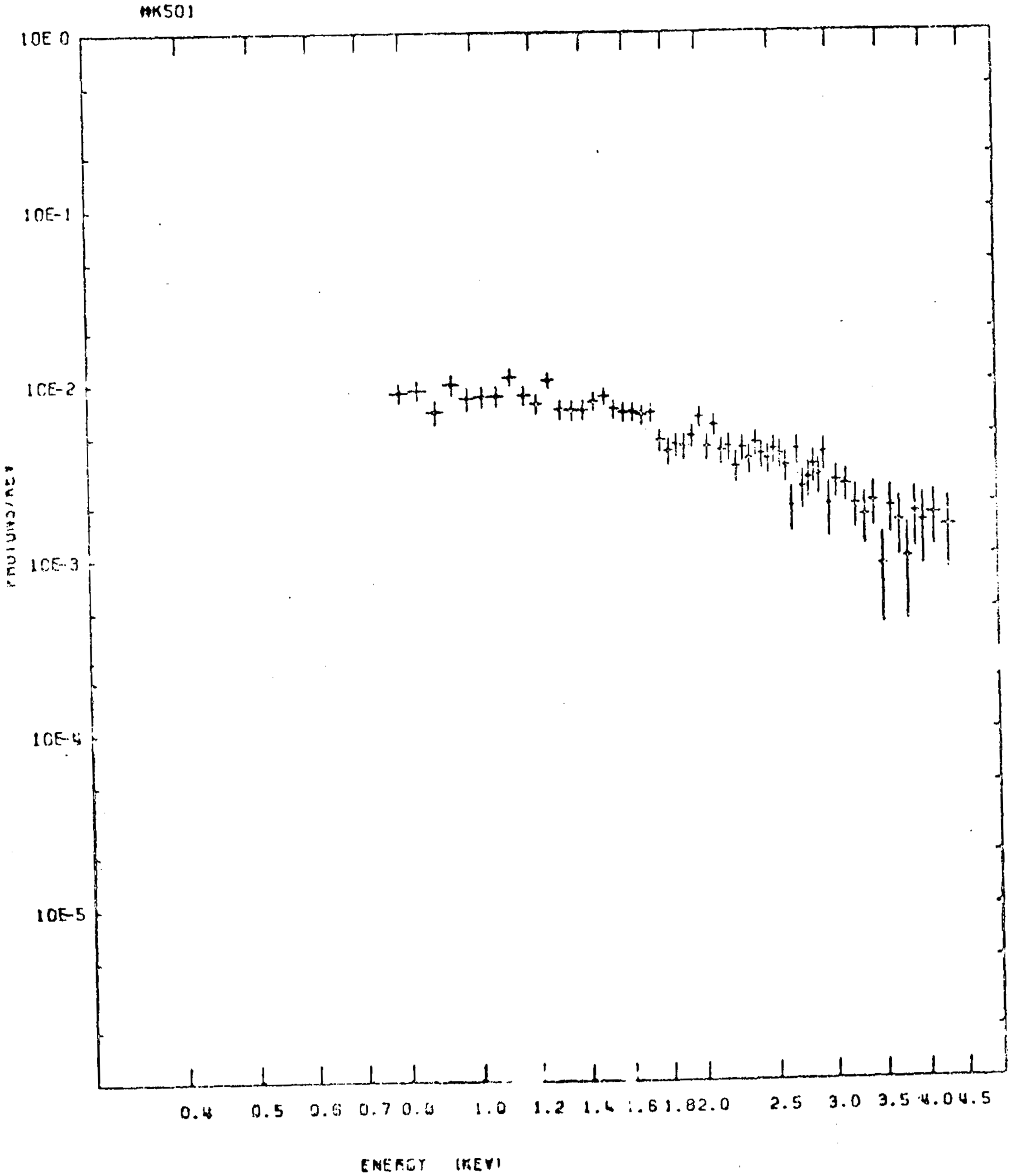
MK501
10E 0
10E-1
10E-2
10E-3
10E-4
10E-5
PHOTONS/CM2/S/KEV
0.4
0.5
0.6
0.7
0.8
1.0
1.2
1.4
1.6
1.8
2.0
2.5
3.0
3.5
4.0
4.5
ENERGY (KEV)

Figure 20

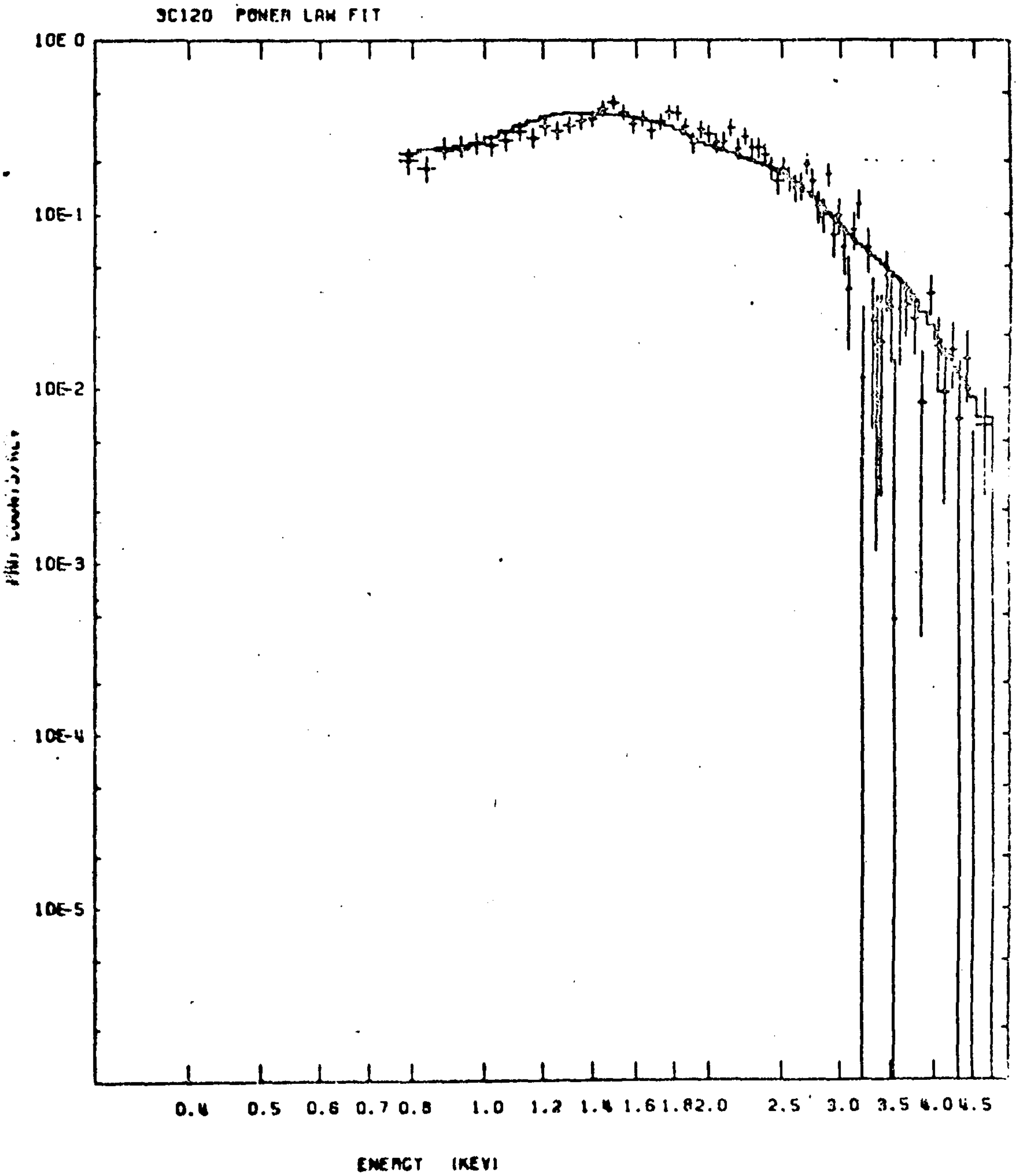

3C120 POWER LAW FIT
10E 0
10E-1
10E-2
10E-3
10E-4
10E-5
0.4
0.5
0.6
0.7
0.8
1.0
1.2
1.4
1.6
1.8
2.0
2.5
3.0
3.5
4.0
4.5
ENERGY (KEV)

Figure 21

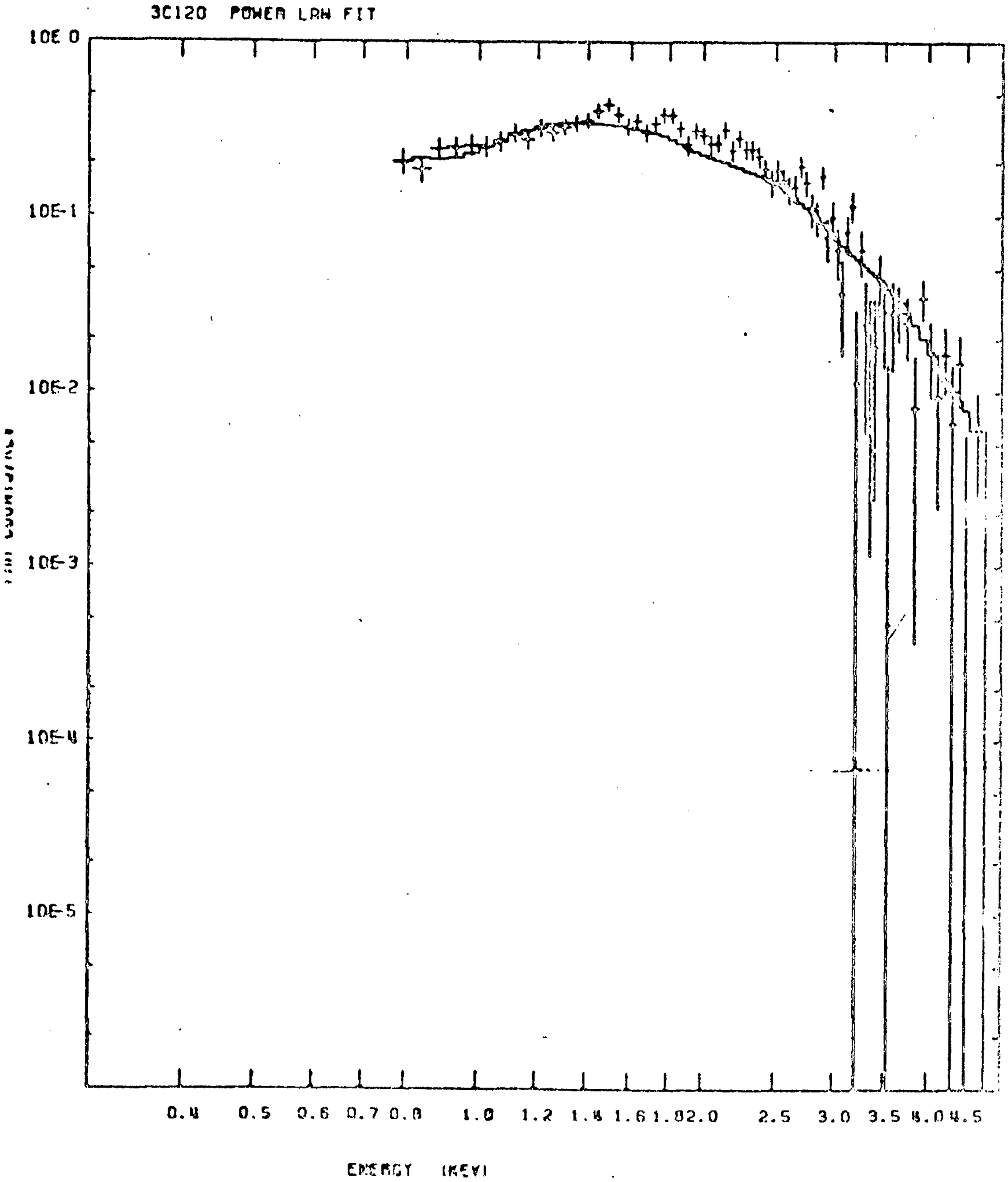
3C120 POWER LAW FIT
10E 0
10E-1
10E-2
10E-3
10E-5
0.4
0.5
0.6
0.7
0.8
1.0
1.2
1.4
1.6
1.8
2.0
2.5
3.0
3.5
4.0
4.5
ENERGY (KEV)

Figure 22

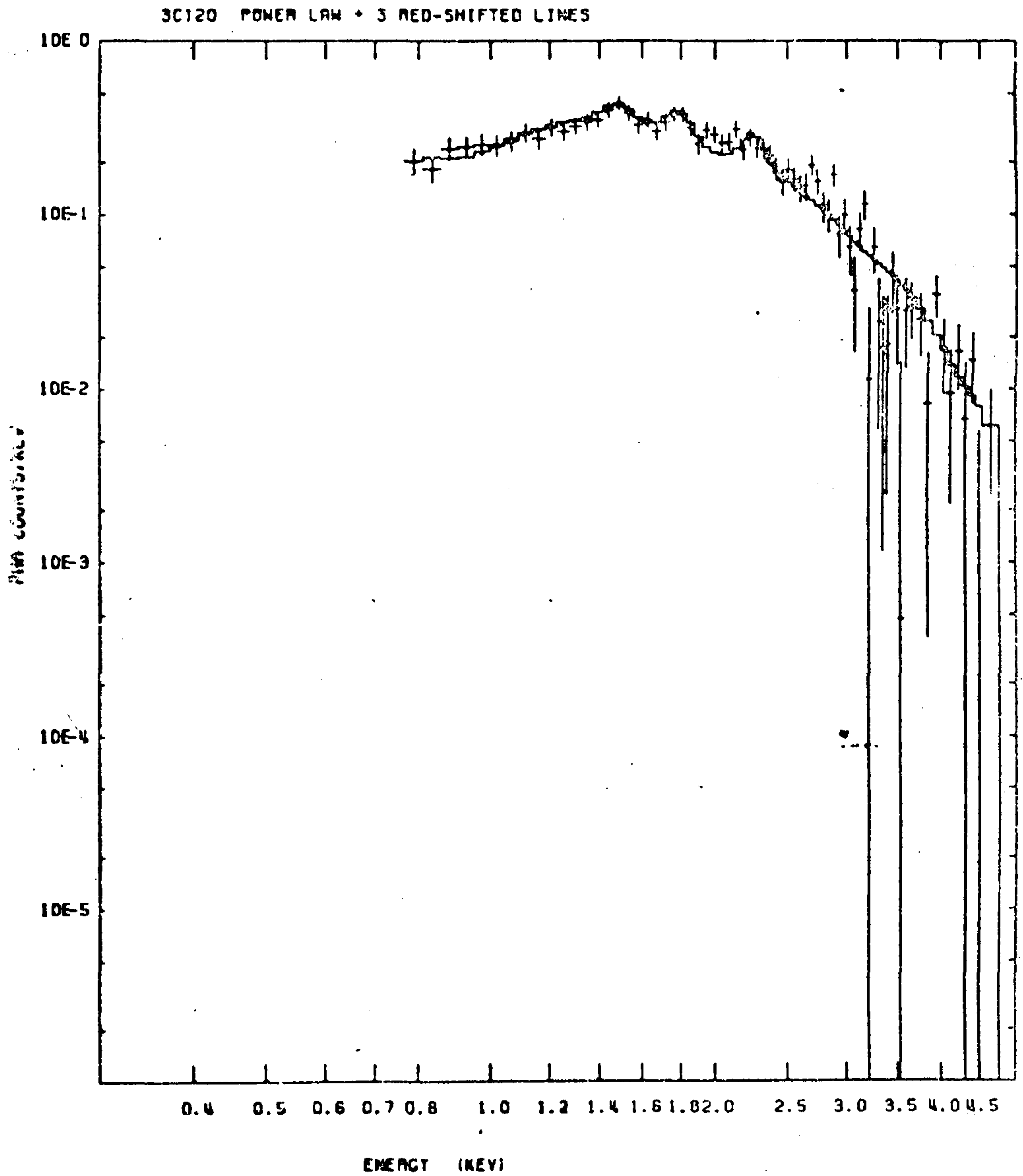
3C120 POWER LAW + 3 RED-SHIFTED LINES
10E 0
10E-1
10E-2
10E-3
10E-4
10E-5
0.4
0.5
0.6
0.7
0.8
1.0
1.2
1.4
1.6
1.8
2.0
2.5
3.0
3.5
4.0
4.5
ENERGY (KEV)

Figure 23

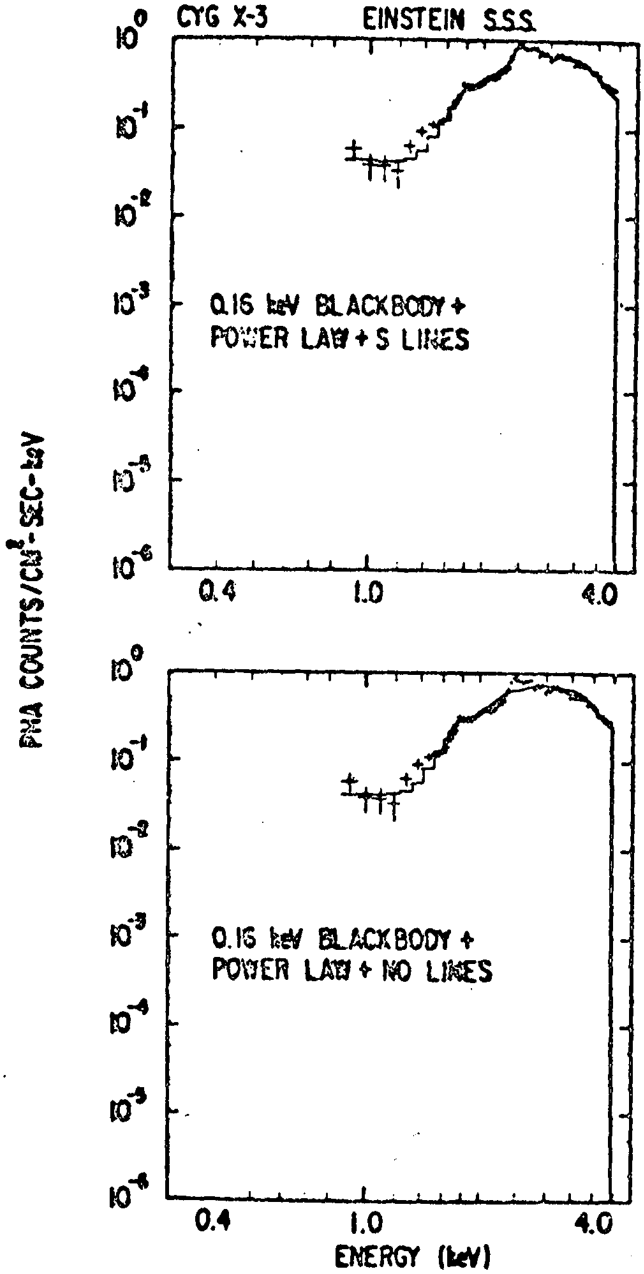
CYG X-3
EINSTEIN S.S.S.
0.16 keV BLACKBODY +
POWER LAW + S LINES
0.16 keV BLACKBODY +
POWER LAW + NO LINES
PHA COUNTS/CM²-SEC-keV
ENERGY (keV)
0.4
1.0
4.0

Figure 24

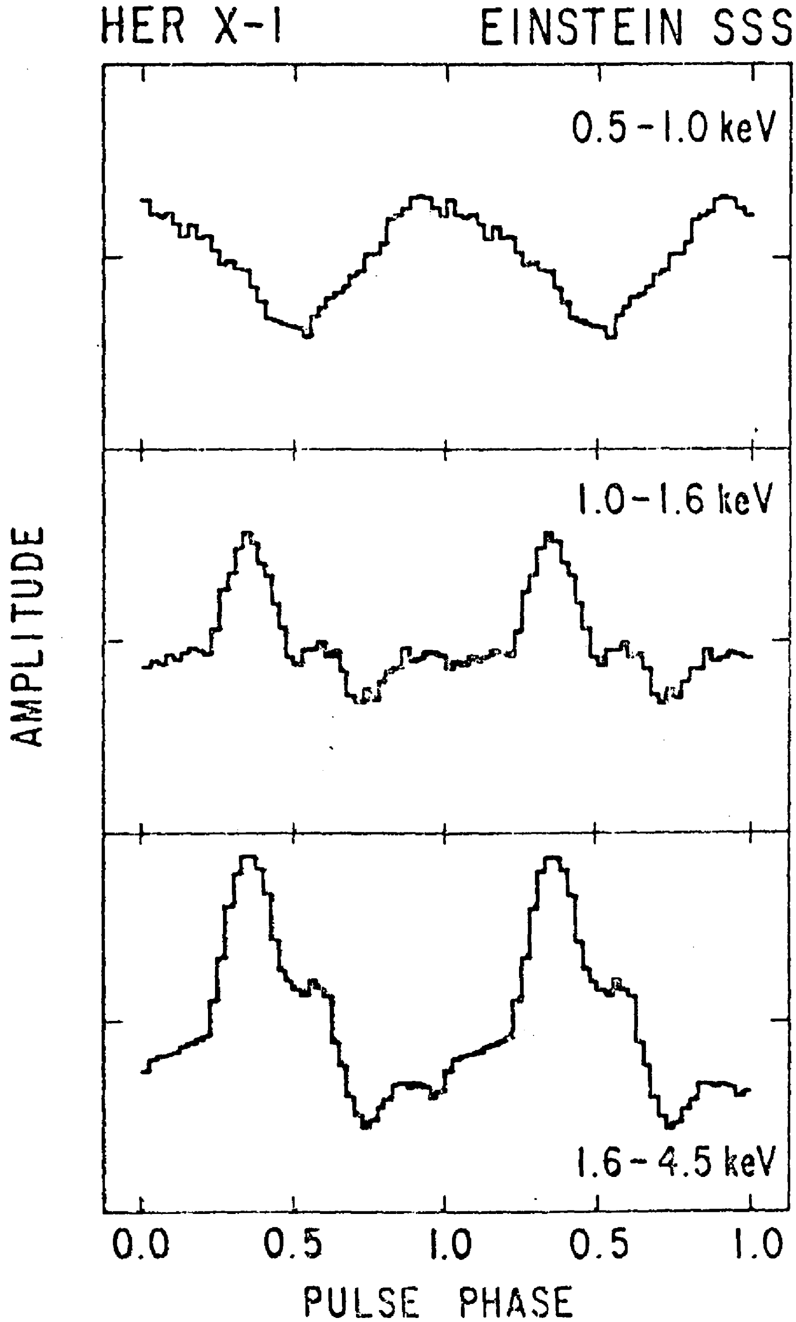

HER X-1
EINSTEIN SSS
0.5 - 1.0 keV
1.0 - 1.6 keV
1.6 - 4.5 keV
AMPLITUDE
0.0
0.5
1.0
0.5
1.0
PULSE PHASE

Figure 25

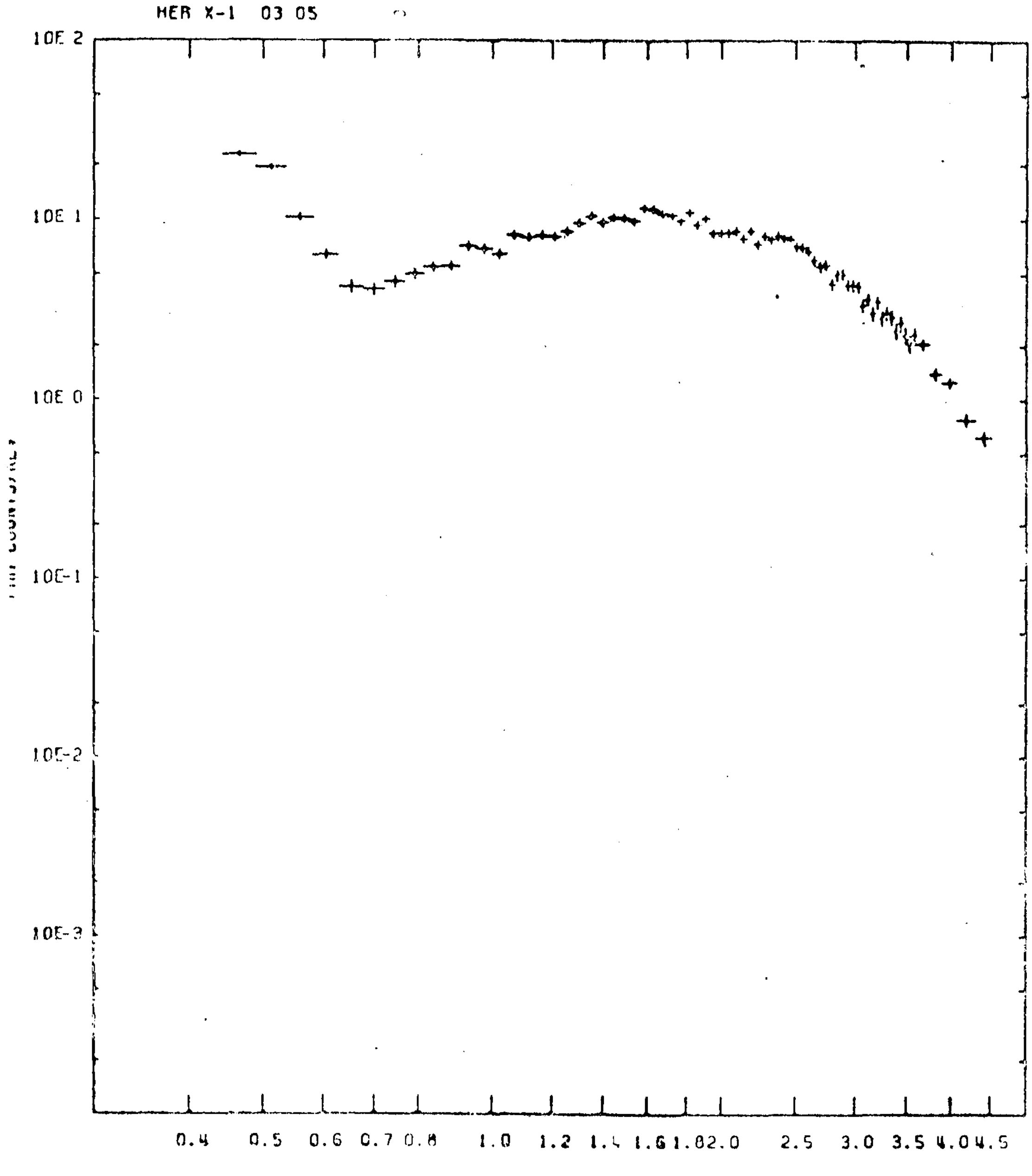
HER X-1 03 05
10E 2
10E 1
10E 0
10E-1
10E-2
10E-3
0.4
0.5
0.6
0.7
0.8
1.0
1.2
1.4
1.6
1.8
2.0
2.5
3.0
3.5
4.0
4.5
ENERGY (KEV)

Figure 26

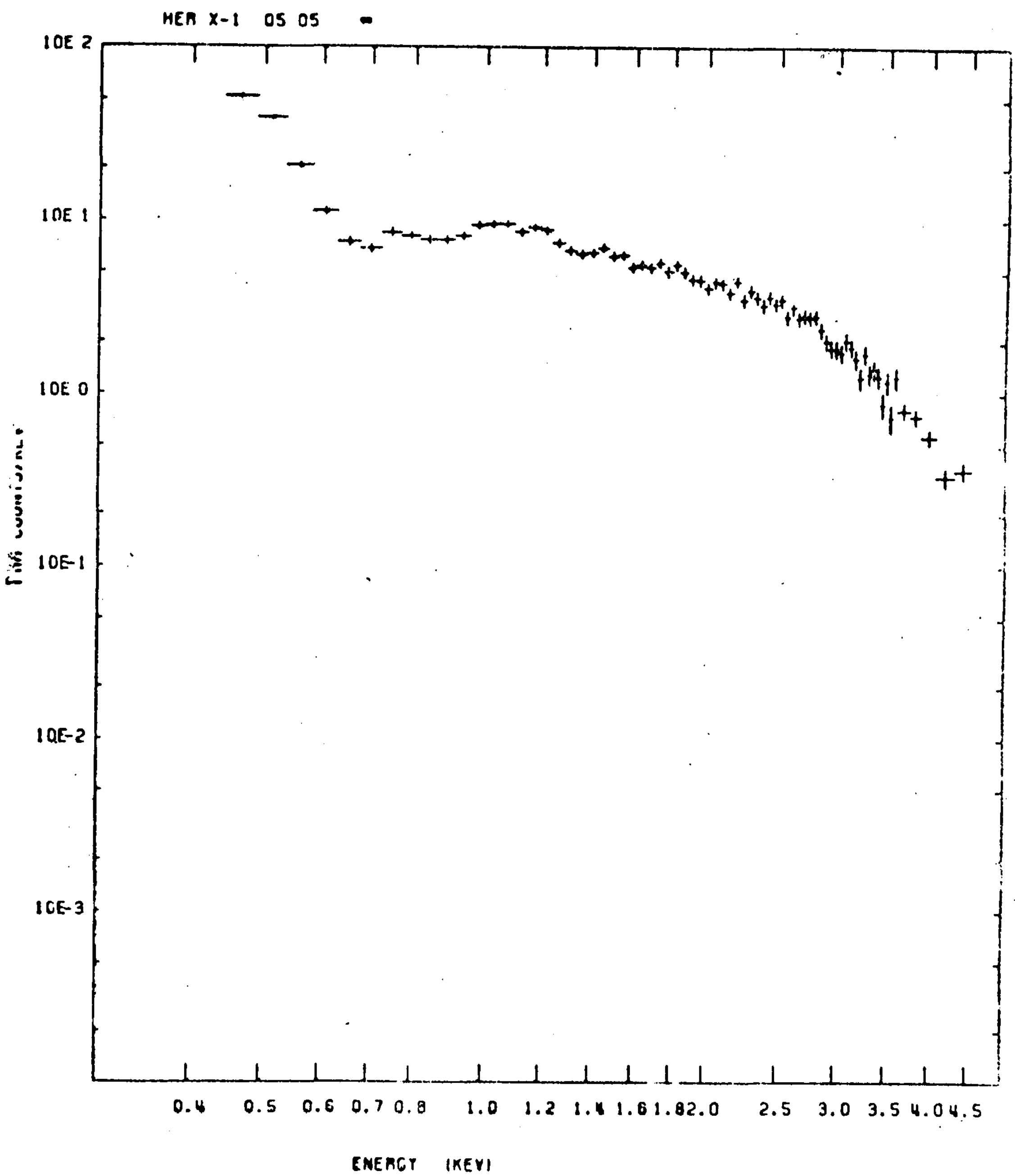

HER X-1 05 05
10E 2
10E 1
10E 0
10E-1
10E-2
10E-3
0.4
0.5
0.6
0.7
0.8
1.0
1.2
1.4
1.6
1.8
2.0
2.5
3.0
3.5
4.0
4.5
ENERGY (KEV)

Figure 27

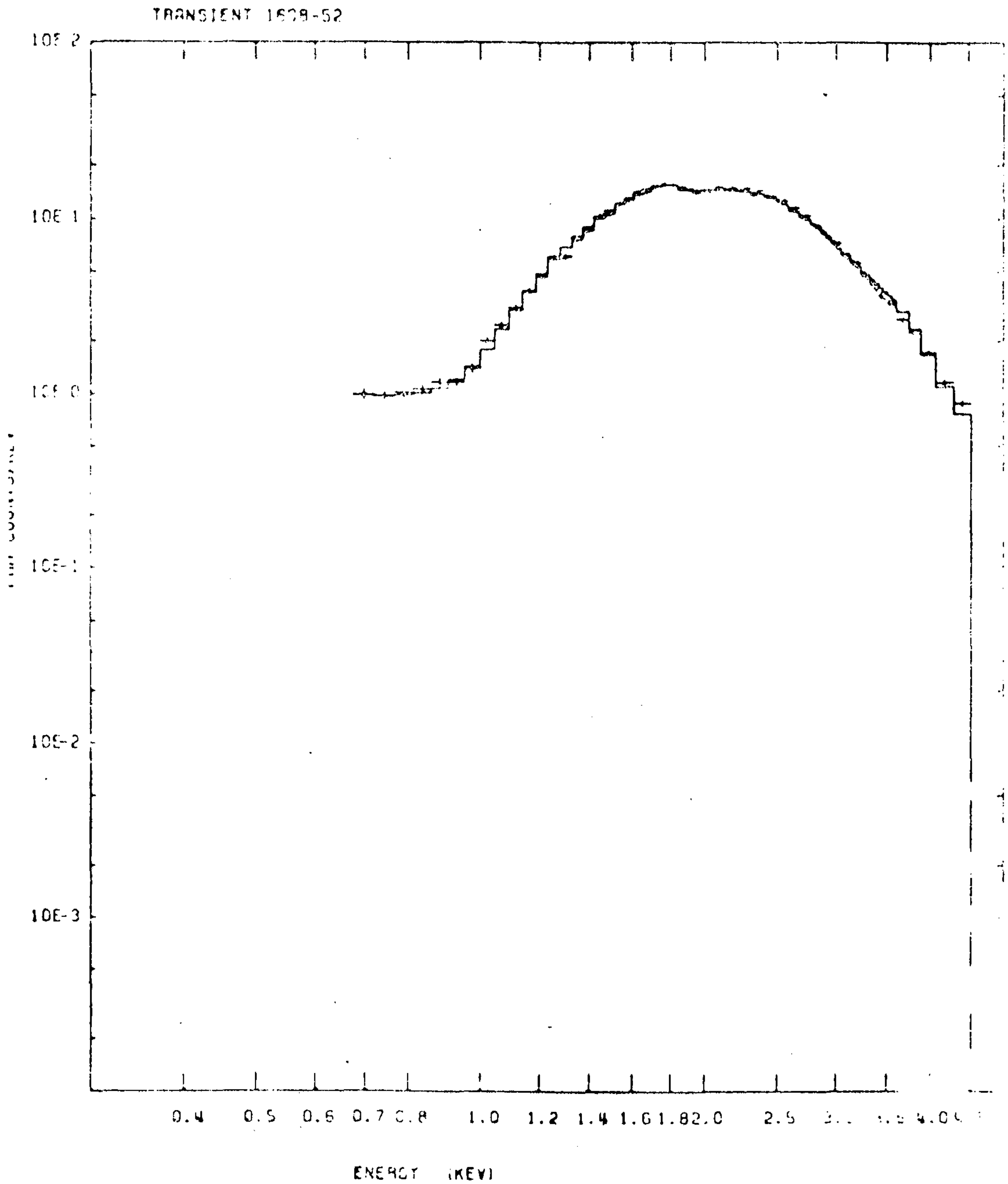
TRANSIENT 1608-52
10E 2
10E 1
10E 0
10E-1
10E-2
10E-3
0.4
0.5
0.6
0.7
0.8
1.0
1.2
1.4
1.6
1.8
2.0
2.5
ENERGY (KEV)

Figure 28

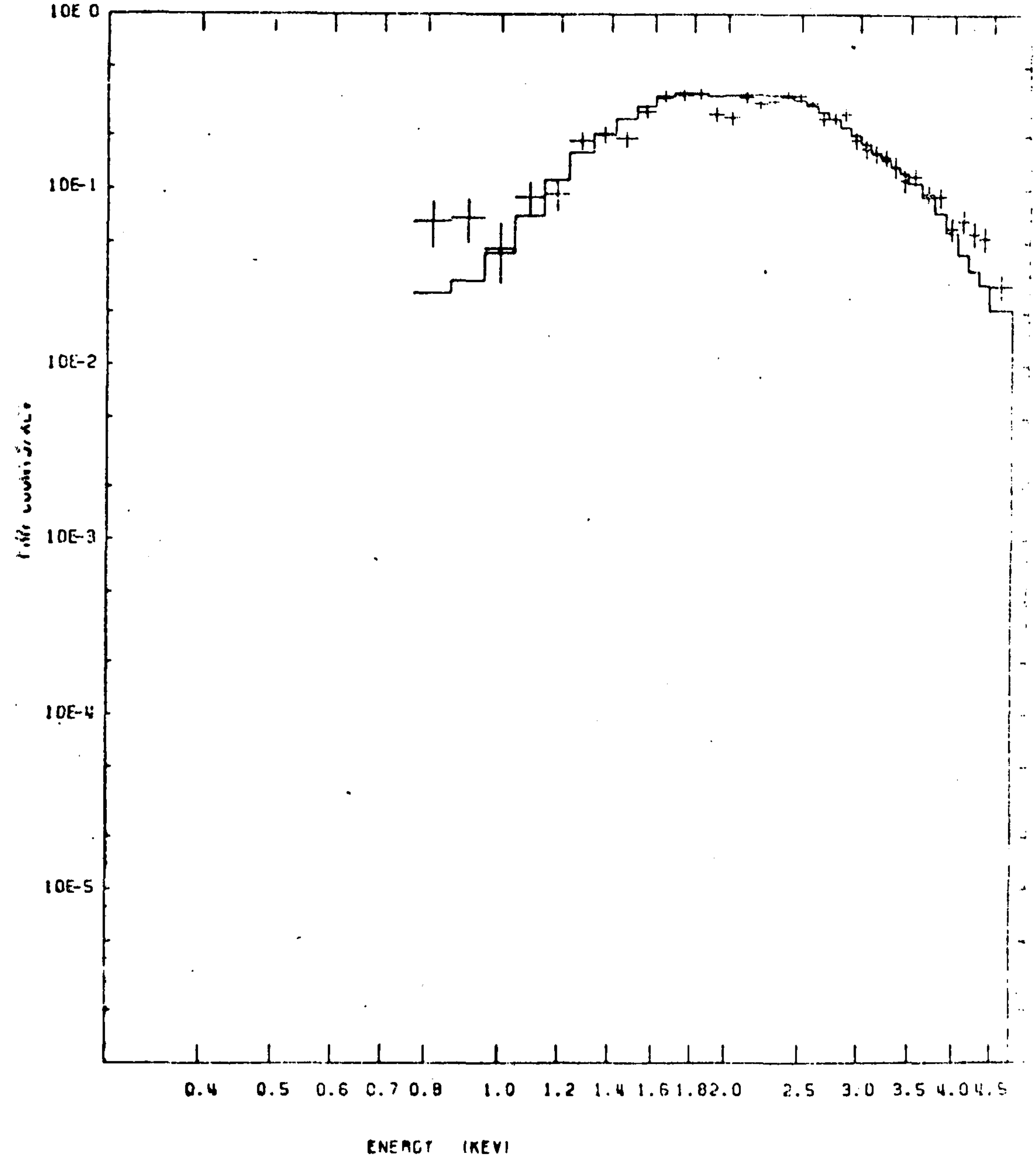

10E 0
10E-1
10E-2
10E-3
10E-4
10E-5
0.4
0.5
0.6
0.7
0.8
1.0
1.2
1.4
1.6
1.8
2.0
2.5
3.0
3.5
4.0
4.5
ENERGY (KEV)

Figure 29